

Collective Effects for eRHIC

G. Wang, A. Fedotov, Y. Hao, V. N. Litvinenko, Y. Luo,
V. Ptitsyn, W. Xu

Outline

- Fast beam-ion instability
 - Analytical calculation from linear theory
 - Numerical simulation: weak-strong
- Multi-bunch beam breakup due to HOM of SRF cavities
- Single bunch beam breakup due to resistive wall
- Energy loss and energy spread due to various effects:
 - Coherent synchrotron radiation
 - wall roughness
 - resistive wall
 - SRF cavities
- Beam losses:
 - scattering with residue gas: elastic scattering, Bremsstrahlung
 - Tousheck effects
- Summary

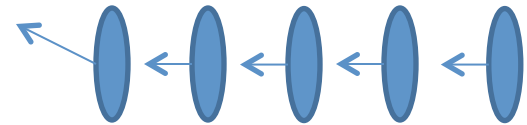
Fast Beam-ion instability: mechanism

s_2

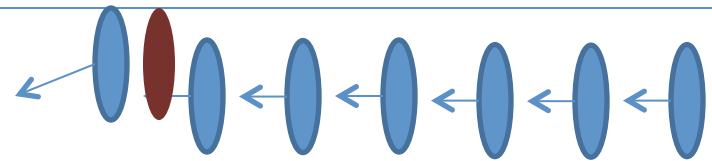
s_1

$s = 0$

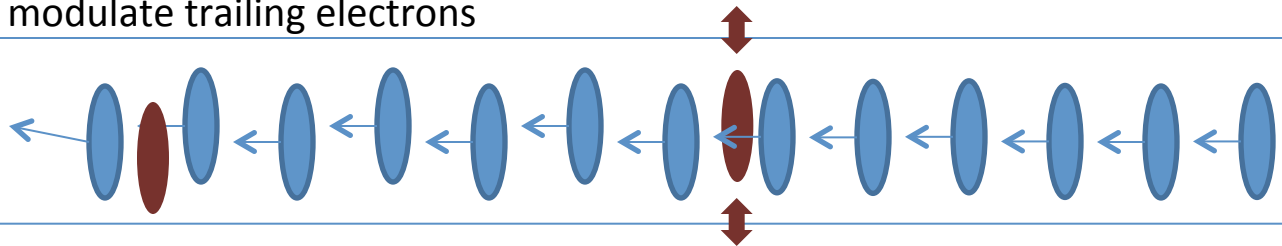
1. Initial transverse velocity due to shot noise



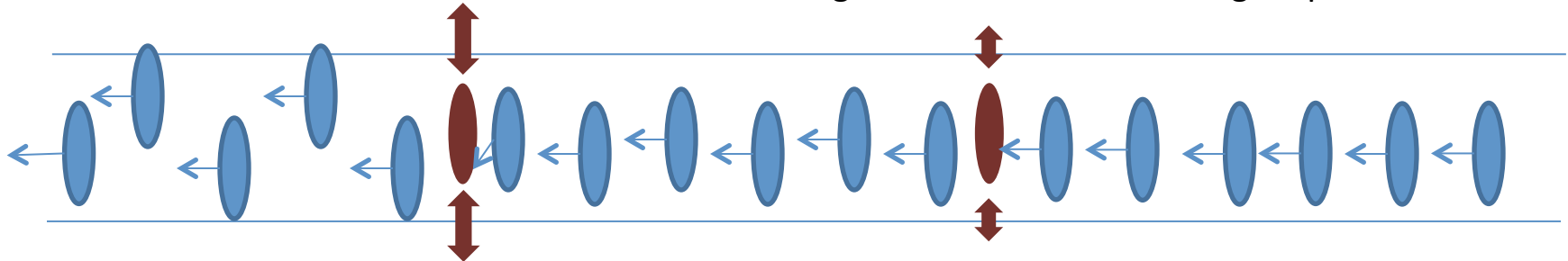
2. Ions are generated with offsets and start to oscillate



3. Ions' oscillation modulate trailing electrons



4. Transverse location modulation at a given s has the ions' oscillating frequency and hence **resonantly** drive ions downstream, which in turn drive the trailing electrons with increasing amplitude -> instability.



eRHIC Parameters and Assumptions

Electron		Residue gas	
Bunch Charge	5.3 nC	Gas species	CO
rf frequency	413 MHz	Gas pressure	1 nTorr
rms emittance	20 mm.mrad	Ion from gas	CO+
Beta function	5 m	Temperature	270K
rep. frequency	9.38 MHz	Ioni. cross-section	1.64 Mbar

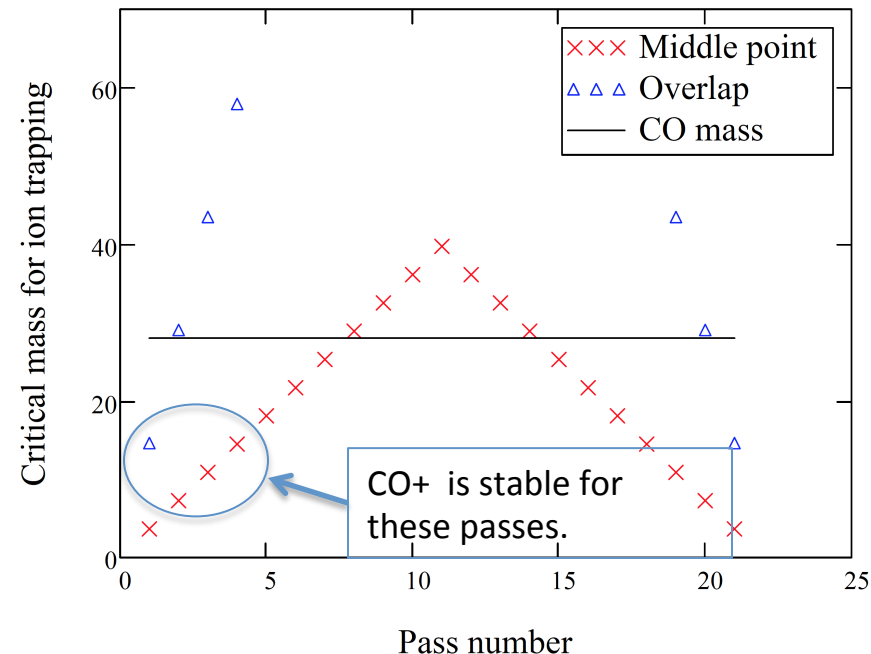
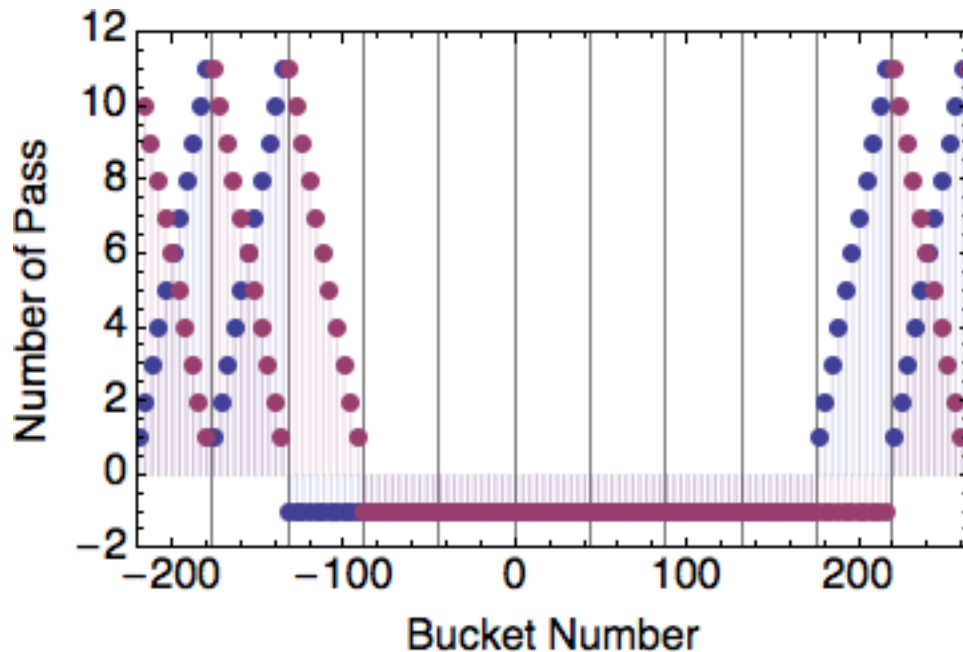
- As a first estimation, I calculate the growth rate inside arc assuming the bunches with different energies are transversly seperated and neglect the effects coming from bunches with different energies.
- I also neglect the neutral gas density variation caused by ionization, assuming the thermal motion is fast enough to replenish the lost neutral gas molecules.
- Currently, we only considered CO as the residue gas species. We plan to include other species such as CO₂ in the future studies.

Ion trapping

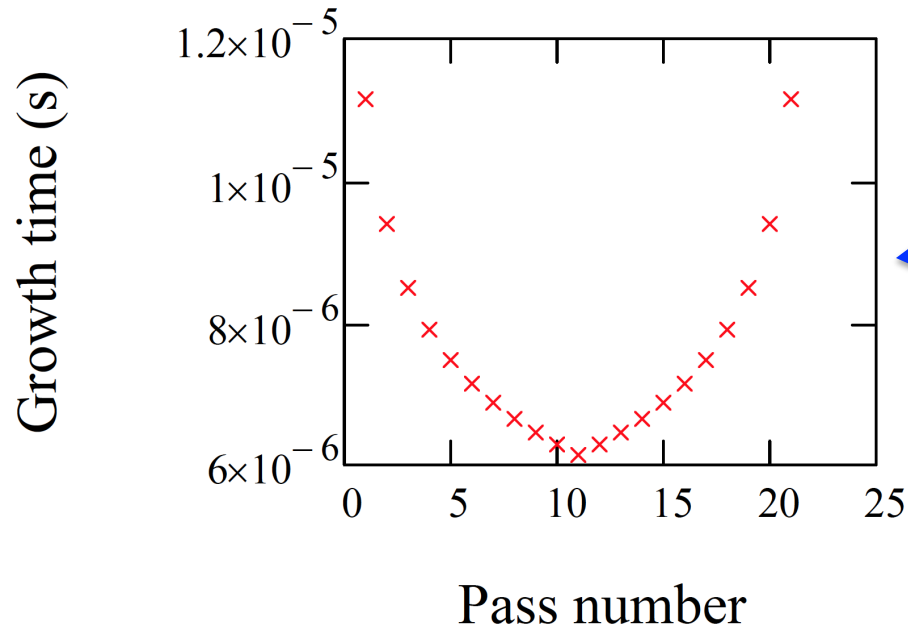
- The stability condition for stable ion motion under the focusing force of electron bunches is given by the following condition:

$$A_{critical} \geq \frac{N_e r_p L_{sep}}{2\sigma_x (\sigma_x + \sigma_y)}$$

- Due to the beam size and bunch pattern, the passes that are possible to trap CO^+ are the lowest 4 energy passes: 0.92 GeV, 1.828 GeV, 2.736 GeV and 3.644 GeV.



FII Linear Theory: Growth Time



Growth time as calculated from

$$\tau_{grow} = \sqrt{\frac{3^{3/2} \gamma_e L_{sep}^{3/2} \sigma_y^{3/2} (\sigma_y + \sigma_x)^{3/2} A^{1/2}}{4c^2 N_e^{3/2} d_{gas} \sigma_{ionization} r_e r_p^{1/2} \beta_x s_{obs}}}$$

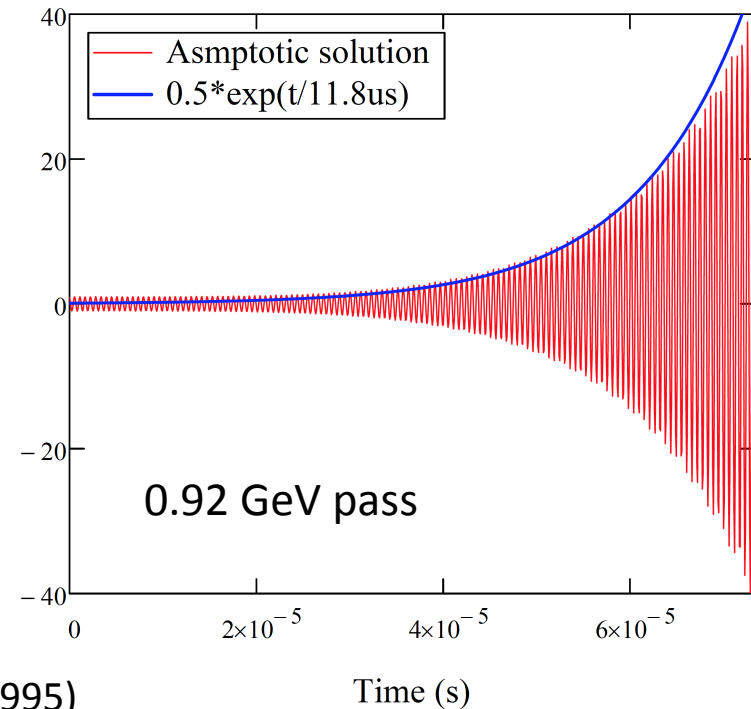
$$s_{obs} = 3833m$$

$$y_b(s, z) = \frac{\hat{y}}{2} \left\{ J_0 \left[2\sqrt{\eta(s, z)} \right] \sin(\omega_i z + \omega_\beta s + \phi + \theta) + I_0 \left[2\sqrt{\eta(s, z)} \right] \sin(\omega_i z - \omega_\beta s - \phi + \theta) \right\}$$

$$\sim e^{t/\tau_{grow}} \quad \text{for } t \gg \tau_{grow}$$

Transverse offsets of electron bunches as they pass through the observation point at s=3833 m.

Tran. offset of the bunches at s=3833m



FII Linear Theory: Saturation of Exponential Growth

- From linear theory, ions will oscillate with greater amplitude before substantial electron oscillation develops. The linear theory breaks when the separation of the centroids of the ions and the electrons become larger than the electron beam size.

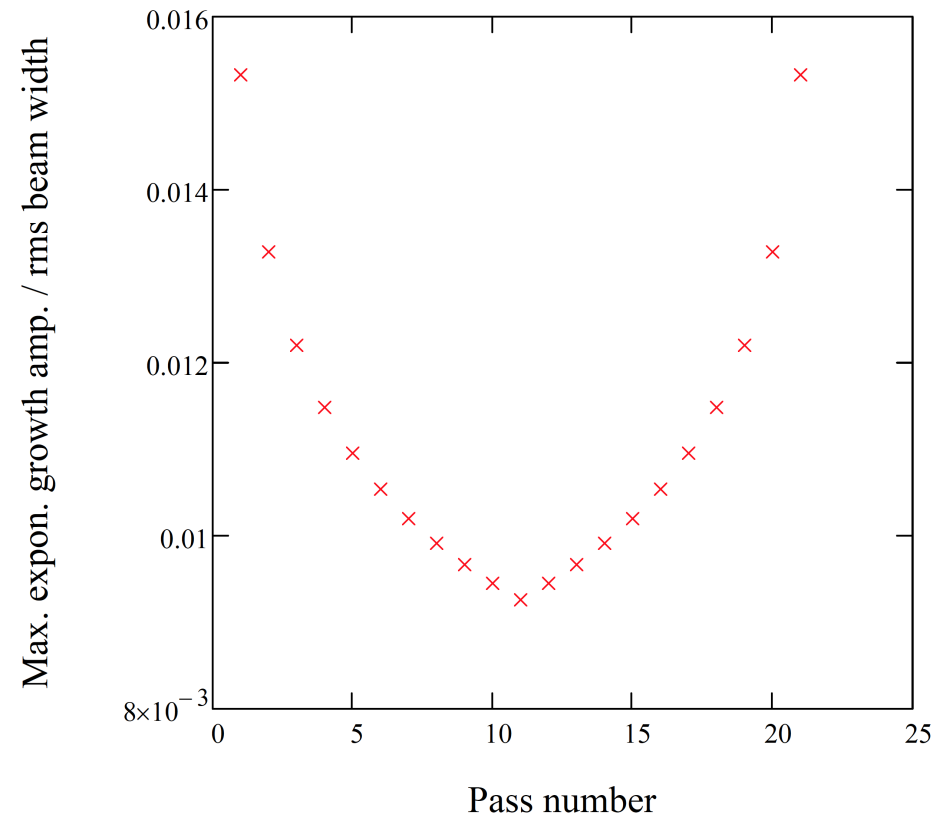
$$y_i / y_b \sim \omega_i / (4c\sqrt{\eta_0})$$

$$\text{for } \omega_\beta s \gg 1 \quad \text{and} \quad \omega_i(z + z_0) \gg 1$$

$$\eta_0 = \frac{N_e^{3/2} d_{gas} \sigma_{ionization} r_e r_p^{1/2} \beta_x s}{3^{3/2} \gamma_e \sigma_y^{3/2} L_{sep}^{3/2} (\sigma_y + \sigma_x)^{3/2} A^{1/2}}$$

- Hence, it is likely that the fast growth predicted by linear theory will saturate at $y_b \ll \sigma_y$

$$y_b / \sigma_y \sim 1.5\% \quad \text{for } 0.92 \text{ GeV energy pass}$$

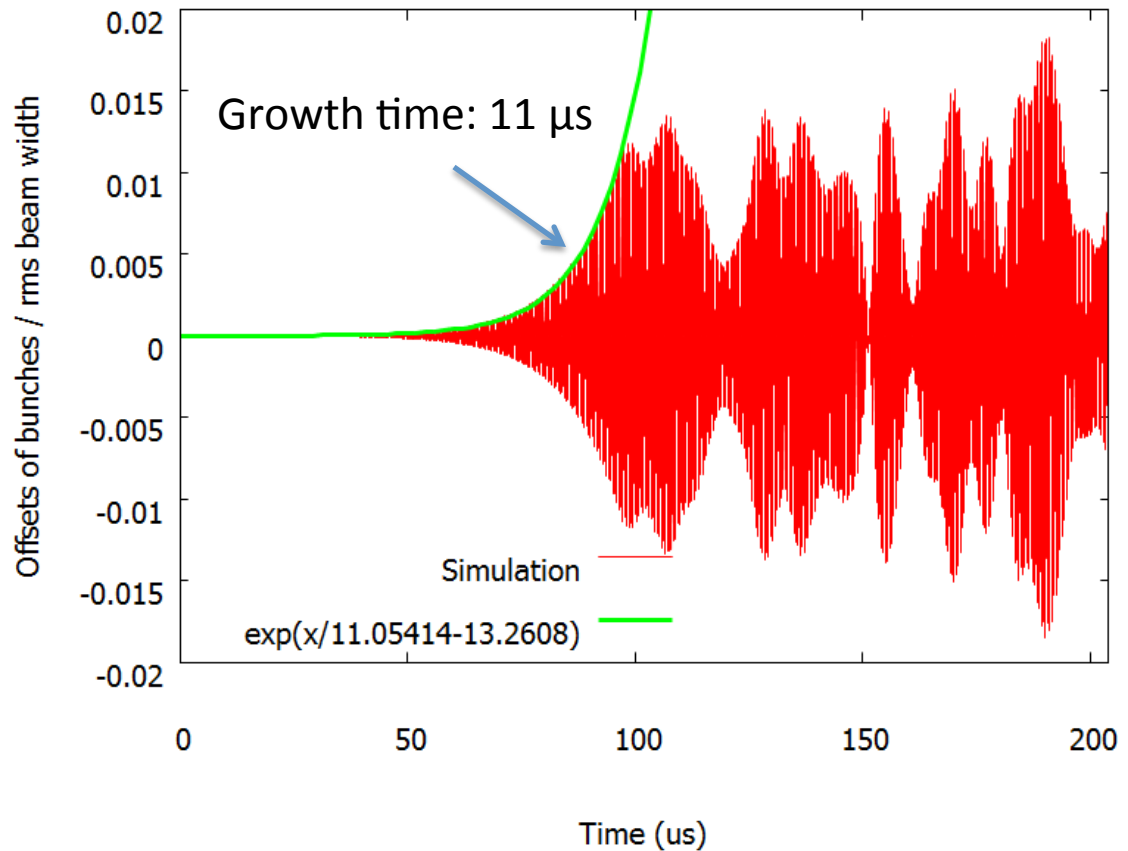


FII Simulation: Description of the Code

- Weak-strong code (written by Y. Luo):
 - Electron bunches are rigid with Gaussian transverse density distribution;
 - Residue gas molecules interact with electrons at given number of locations along the accelerator with optical parameters specified at each location;
 - A given number of macro-ions are generated after each electron bunch passes through the interaction point;
 - Electron bunches are refreshed each turn but ions are kept through the whole simulation.
 - The offsets of the incoming electron bunches are observed at a given location: $s=3833\text{m}$.
- For this preliminary study, we set 10 evenly distributed interaction points, with a constant beta function of 5 meters. The deceleration bunches are put in the middle point of two adjacent accelerating bunches, i.e. the worst case scenario for ion trapping.

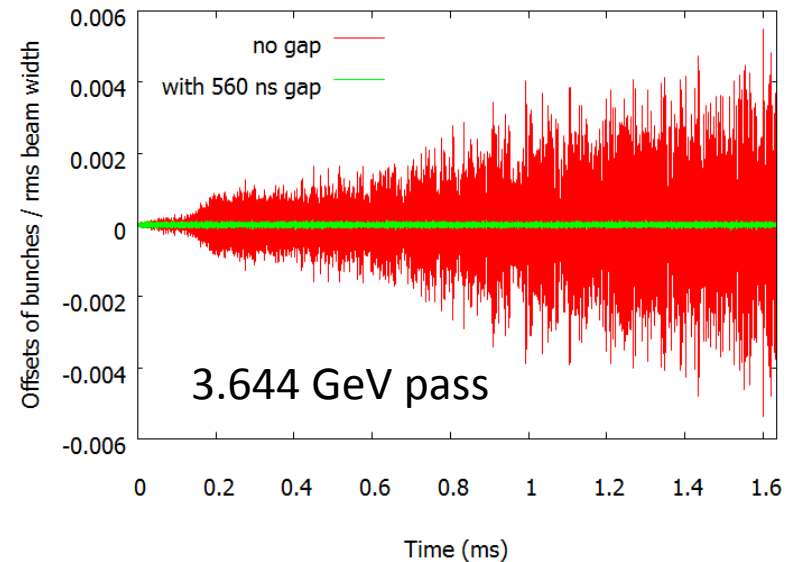
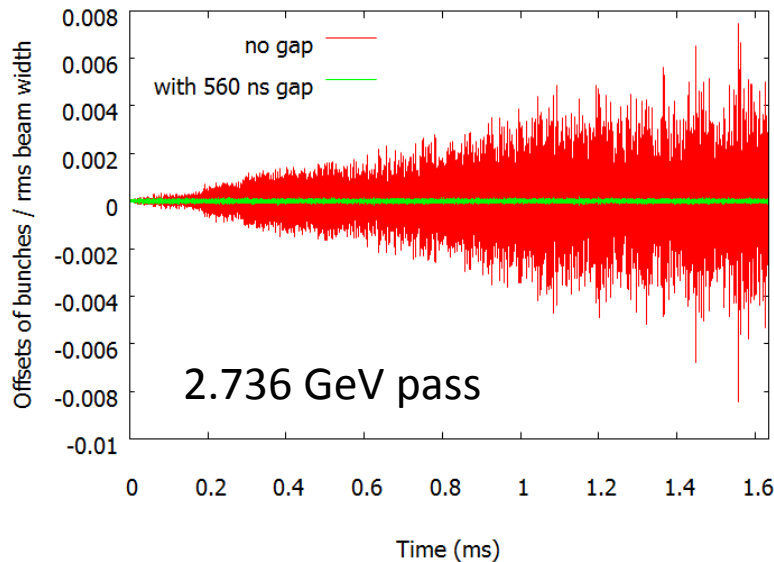
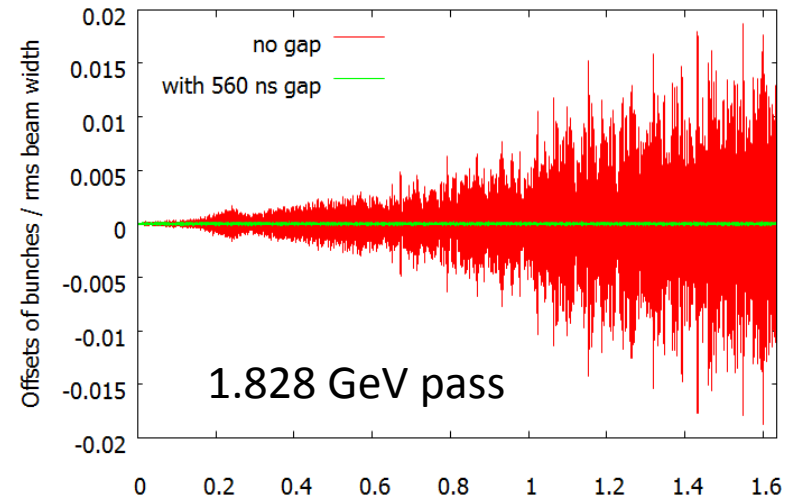
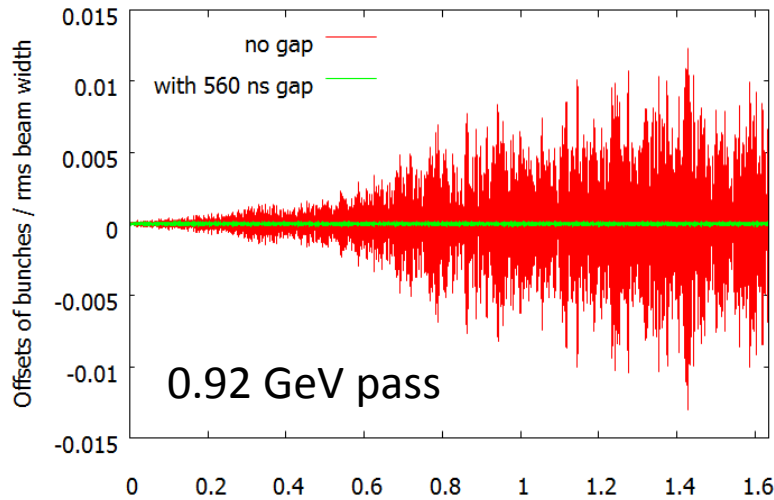
FII Simulation: Checking the Linear Limit

- Artificially putting the freshly created ions inside 0.1 sigma of the electron beam.
- The growth time is 11 μs , which agree with the prediction from the linear theory, i.e. 11.8 μs .
- The exponential growth stops at $\sim 1.3\%$ of rms beam width, which is close to the prediction of linear theory, $\sim 1.5\%$.



FII Simulation Results

(Assuming Constant Neutral Gas Pressure)

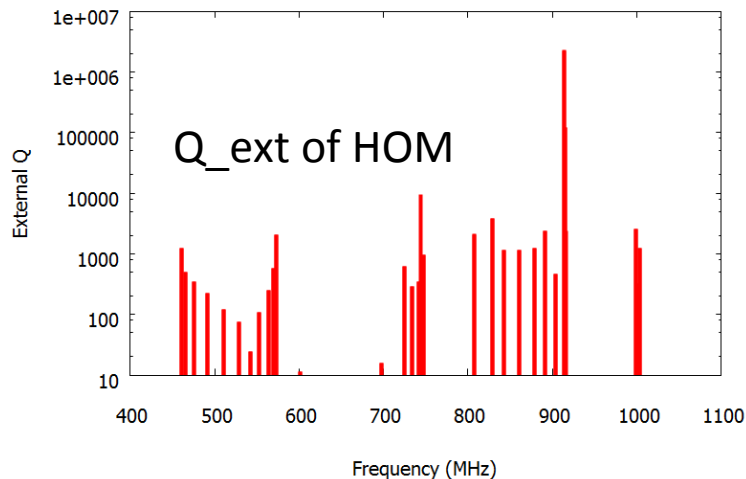
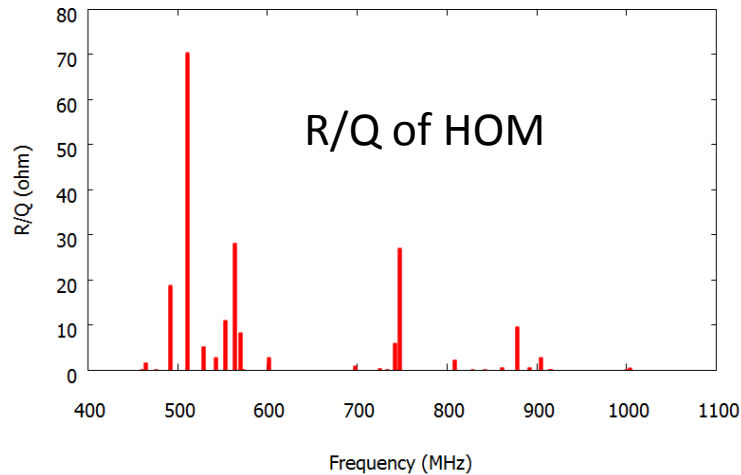


- Non-linear space charge effects reduce both the initial growth rate and the the amplitude at saturation. But without gap, the oscillation amplitude increases persistently.

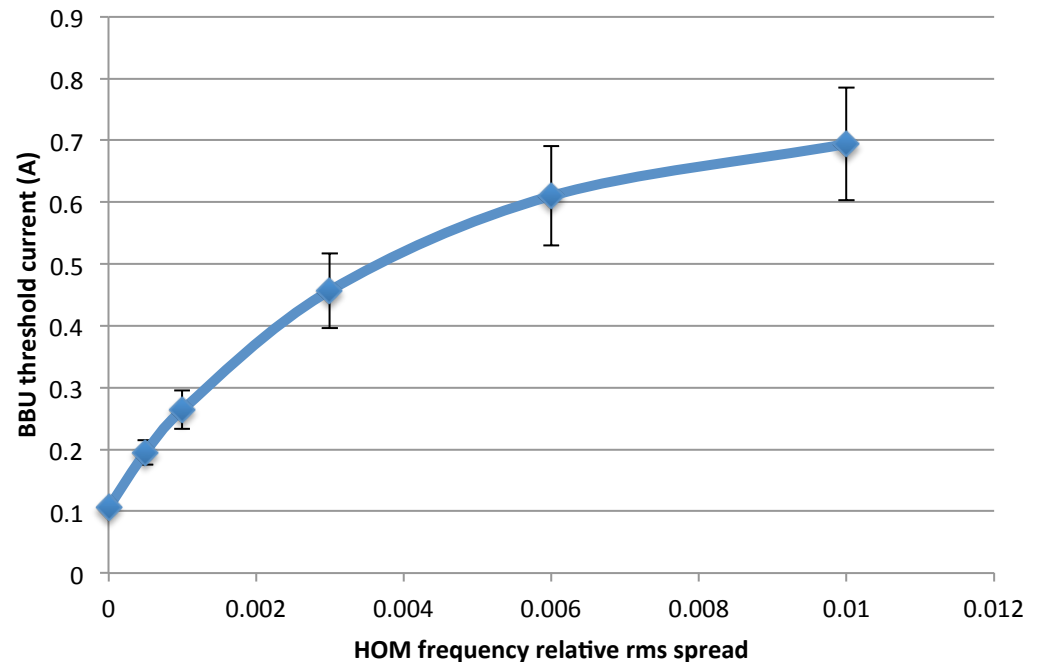
Summary for Fast Ion Instability Studies

- Without a gap in the electron bunch pattern, the linear theory predicts the growth time for fast ion instability is $6 \sim 11 \mu\text{s}$ with the saturation amplitude of 0.015σ .
- Numerical simulation shows that although Landau damping due to non-linear space charge is significant, a slow increase of electron bunch oscillation amplitude persists.
- It is observed from simulation that a 560 ns gap in the electron bunch train completely suppressed the instability.
- Complete simulation connecting all 20 passes is work in progress.

Multi-bunch BBU due to HOM of Cavities

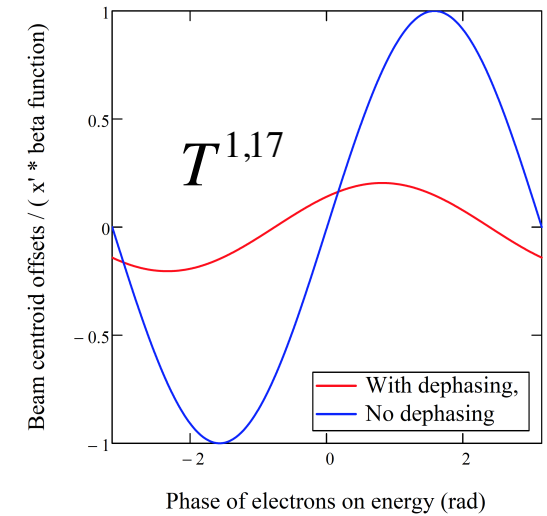
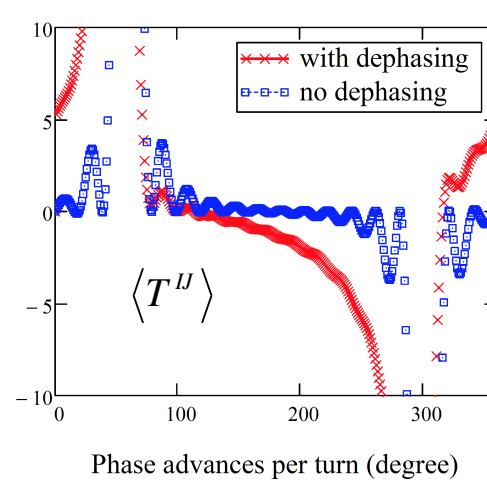
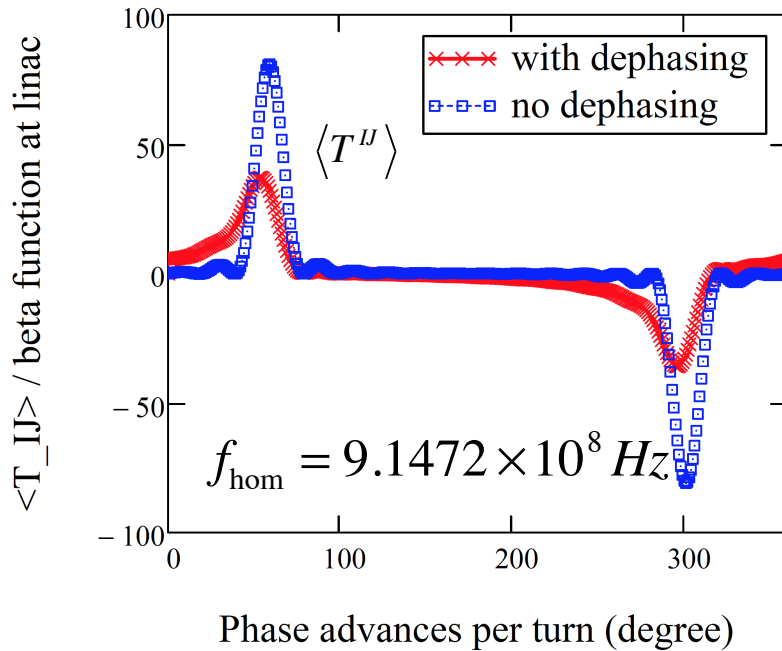


- BBU threshold current are found by simulation with code written by E. Pozdeyev.
- Even without HOM frequency variation, the threshold current, 106 mA, is more than a factor of 2 above the designed current, 50 mA.
- With rms HOM frequency variation of 3E-3, the BBU threshold current is 457 mA, a factor of 9 above the designed current.



Courtesy of Y. Hao and W. Xu

Effects of Chromatic Dephasing to Multi-bunch BBU



$$I_{th} = -\frac{2c^2}{eR_g Q \omega} \frac{1}{\langle T_{II} \rangle} \quad \langle T_{II} \rangle \equiv \sum_{J=1}^{2N} \sum_{I=J+1}^{2N} T_{II} \sin[\omega_{\text{hom}}(t_I - t_J)]$$

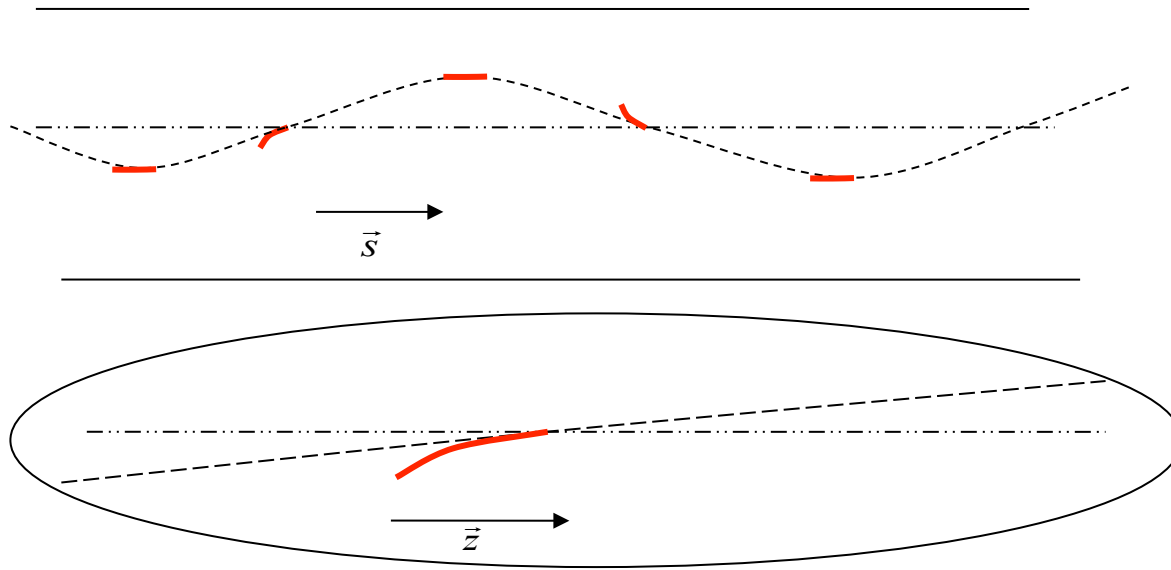
$$f(\delta) = \frac{1}{\sqrt{\pi} k \sigma_z} \cdot \frac{1}{\sqrt{-\delta}} \exp\left(\frac{\delta}{k^2 \sigma_z^2}\right) \text{ for } \delta \leq 0 \quad T_{II} = \frac{w_{i0}^2}{\sqrt{2}} \left\{ \left[\frac{\sqrt{1 + (k^2 \sigma_z^2 \phi_{II})^2} + 1}{1 + (k^2 \sigma_z^2 \phi_{II})^2} \right]^{\frac{1}{2}} \sin(\Delta\psi_{II}) + \left[\frac{\sqrt{1 + (k^2 \sigma_z^2 \phi_{II})^2} - 1}{1 + (k^2 \sigma_z^2 \phi_{II})^2} \right]^{\frac{1}{2}} \cos(\Delta\psi_{II}) \right\}$$

- I only consider energy spread coming from rf curvature, which has substantially smaller reduction of beam response than that of Gaussian energy spread.
- For ~ 3200 accumulated chromaticity after 17 passes, the response is reduced by a factor of 5.
- For a specific HOM considered and identical phase advances for all passes, the dephasing should increase the BBU threshold by a factor of two around 300 degree phase advances while decreasing it in some other ranges of one turn phase advances.
- We plan to include energy spread from other sources and do numerical simulations with chromatic effects taken into account in the next step.

Summary for Multi-bunch BBU

- Even in the absence of HOM variation among cavities and chromatic dephasing due to beam energy spread, BBU threshold is found to be 106 mA, more than a factor of 2 above the designed current.
- For HOM variation of $3\text{E-}3$ level, the threshold increases to 457 mA, a factor of 9 above the designed current.
- Chromatic dephasing can reduce the beam centroid response to HOM kick and its effects to BBU threshold is currently under study.

Single Bunch Beam Breakup due to Wakefield of Resistive Wall



- Each bunch is treated as a string with no transverse size.
- Continuous focusing is assumed for simplicity.
- Betatron tune spread along the bunch is not considered.
- We assume a circular beam pipe with 2 cm diameter, which gives a rough estimation for the vertical plane BBU. The horizontal single bunch BBU involves the complication due to the off-centered orbits for most of the energy passes and we leave it for the future studies.

References:

1. A. W. Chao, B. Richer and C. Yao, NIM 178 (1980) 1-8
2. A. W. Chao, Physics of Collective Beam Instabilities in High Energy Accelerators
3. G. J. Caporaso, W. A. Barletta and V. K. Neil, Particle Accelerators, 11 (1980) 71-79
4. J. R. Delayen, Proceedings of the 2001 Particle accelerator Conference, p. 1865-1867

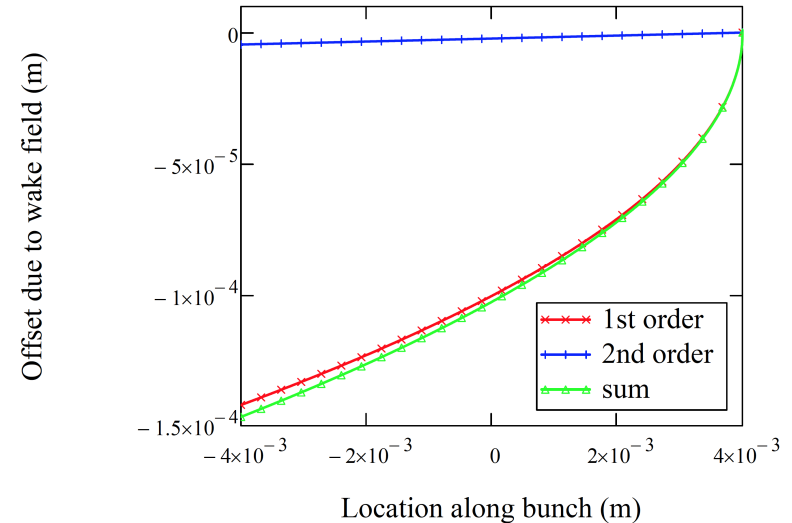
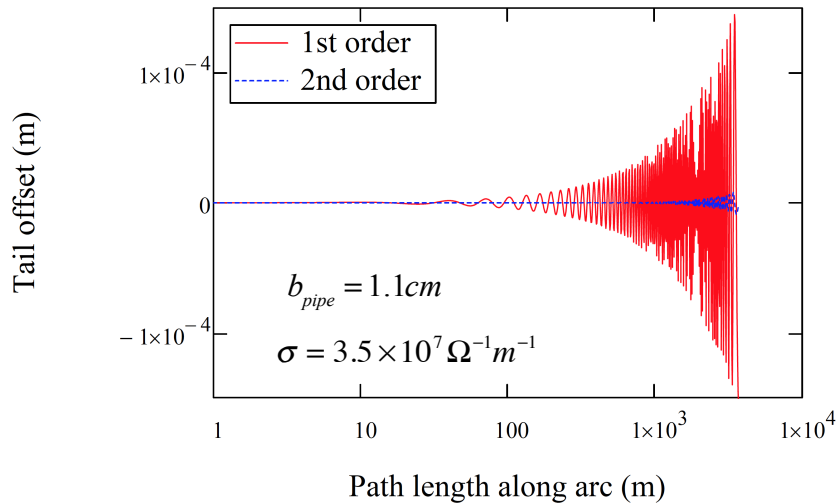
Outside the Linac

$$x^{(0)}(z, s) = d_0(z) \cos(k_0 s) + \frac{d_0'(z)}{k_0} \sin(k_0 s)$$

$$G(s, s') = \frac{\sin[k_0(s - s')]}{k_0}$$

$$x^{(n)}(z, s) = \frac{1}{\pi^{3/2} b^3} \frac{e^2}{m_e c^2 \gamma_i} \int_0^s ds' G(s, s') \int_z^\infty dz' \rho(z') \sqrt{\frac{c}{\epsilon_0 \sigma(z' - z)}} x^{(n-1)}(z', s')$$

$$\rho(z) = \begin{cases} N / l_b, & |z| < \frac{l_b}{2} \\ 0, & \text{otherwise} \end{cases}$$



For the parameters we considered, 1st order solution looks good enough

$$x^{(1)}(z, s) = \frac{1}{\pi^{3/2} b^3} \frac{e^2 N}{2 m_e c^2 \gamma_i k_0 l_b} \sqrt{\frac{c}{\epsilon_0 \sigma}} \left\{ s \sin(k_0 s) \int_z^\infty d_0(z') (z' - z)^{-\frac{1}{2}} dz' - \frac{1}{k_0} \left[s \cos(k_0 s) - \frac{1}{k_0} \sin(k_0 s) \right] \int_z^\infty d_0'(z) (z' - z)^{-\frac{1}{2}} dz' \right\}$$

In Linac

$$\frac{d^2}{du^2} x(z, u) + \frac{1}{u} \frac{d}{du} x(z, u) + \left(\frac{2\pi}{\alpha \lambda_x(z, u)} \right)^2 x(z, u) = \frac{-e^2}{m_e c^2 \gamma_i \alpha^2 u} \int_z^\infty dz' \rho(z') W_1(z' - z) x(z', u)$$

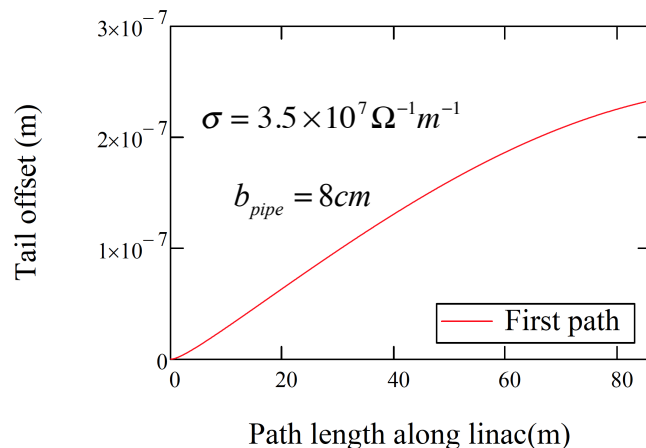
$$u \equiv 1 + \alpha s$$

Using iterative/perturbative method

$$x^{(0)}(z, u) = A J_0 \left(\frac{k_0}{\alpha} u \right) + B Y_0 \left(\frac{k_0}{\alpha} u \right) \quad G(u', u) = \frac{\pi u'}{2} \left\{ J_0 \left(\frac{k_0}{\alpha} u' \right) Y_0 \left(\frac{k_0}{\alpha} u \right) - J_0 \left(\frac{k_0}{\alpha} u \right) Y_0 \left(\frac{k_0}{\alpha} u' \right) \right\}$$

$$x^{(n)}(z, u) = \frac{-e^2}{m_e c^2 \gamma_i \alpha^2} \int_z^\infty dz' \rho(z') W_1(z' - z) \int_1^u G(u', u) x^{(n-1)}(z', u') \frac{1}{u'} du'$$

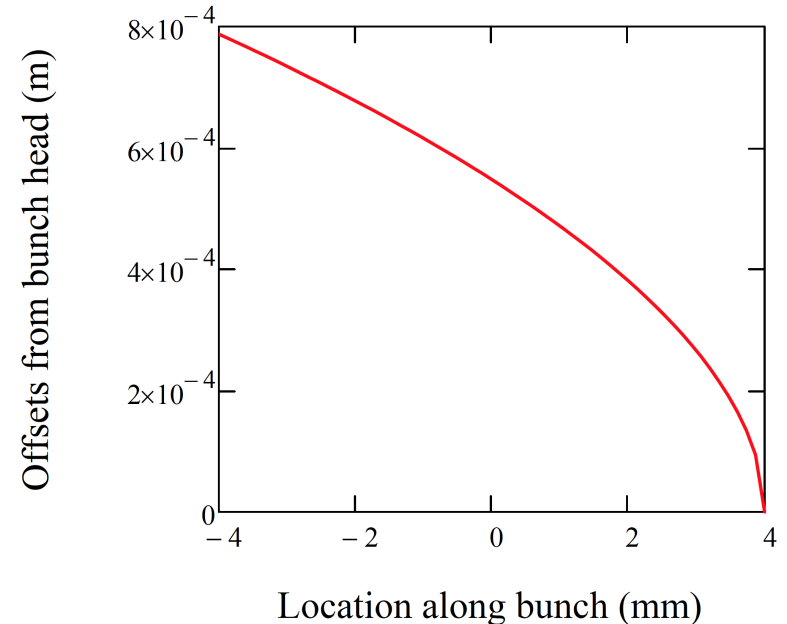
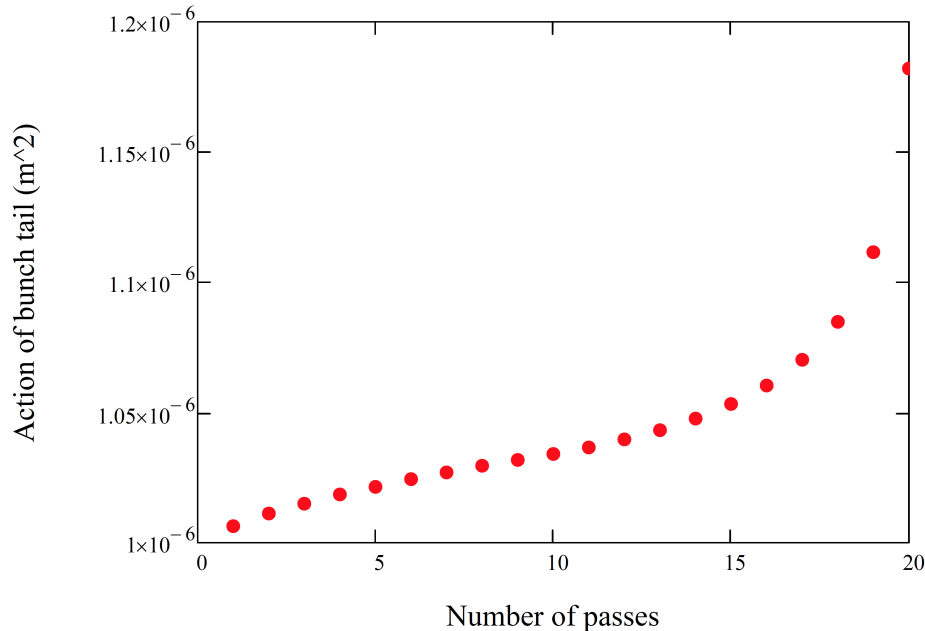
$$x^{(1)}(z, u) = \frac{-e^2 \pi}{2 m_e c^2 \gamma_i \alpha^2} \int_z^\infty dz' \rho(z') W_1(z' - z) \int_1^u \left[J_0 \left(\frac{k_0}{\alpha} u' \right) Y_0 \left(\frac{k_0}{\alpha} u \right) - J_0 \left(\frac{k_0}{\alpha} u \right) Y_0 \left(\frac{k_0}{\alpha} u' \right) \right] \left[A J_0 \left(\frac{k_0}{\alpha} u' \right) + B Y_0 \left(\frac{k_0}{\alpha} u' \right) \right] du'$$



- Thus, we ignore the contribution from Linacs. However Zeor-th order may still play a role, which will be included in the future studies.

Estimation for 20 passes

- Linac is treated as a unit matrix with instant energy jump.



- The tail amplitude increases 18% after 20 passes of the ring.
- The wake field also causes phase difference between head and tail, leading to additional difference in transverse offset along the bunch (~80 % of the initial offset for the considered parameters).

Summary for Single Bunch Vertical BBU due to Resistive Wall

- Assuming a round Aluminum beam pipe with 2 cm diameter, analytical calculation shows that the oscillation amplitude of the electron bunch tail increases by 18 % after 20 passes of the ring due to the transverse resistive wall wake field.
- The estimated effects of vertical BBU due to resistive wall wake looks tolerable.
- Studies for more realistic elliptical beam pipe is under way.
- Similar effects in the horizontal plane will be studied in the future, which involves the effects due to the off-centered orbits for most of the energy passes.

Energy Losses and Energy Spread due to Resistive Wall and RF cavity wake

413 MHz linac HOMs
 $k_{\text{loss}} = 2.03 \text{ V/pC}$
 (per cavity)

$$W_{\parallel}(s) = -\frac{1}{q} \int_{-\infty}^{\infty} dz E_z \left(r_{\text{beam}}, r_{\text{exciting charge}}, z, t = \frac{z+s}{c} \right)$$

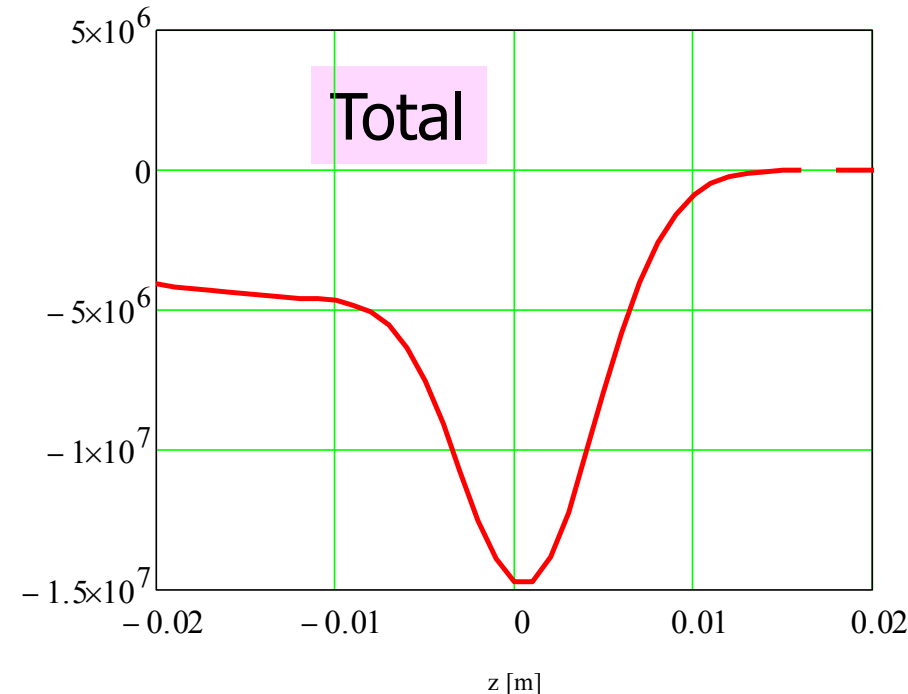
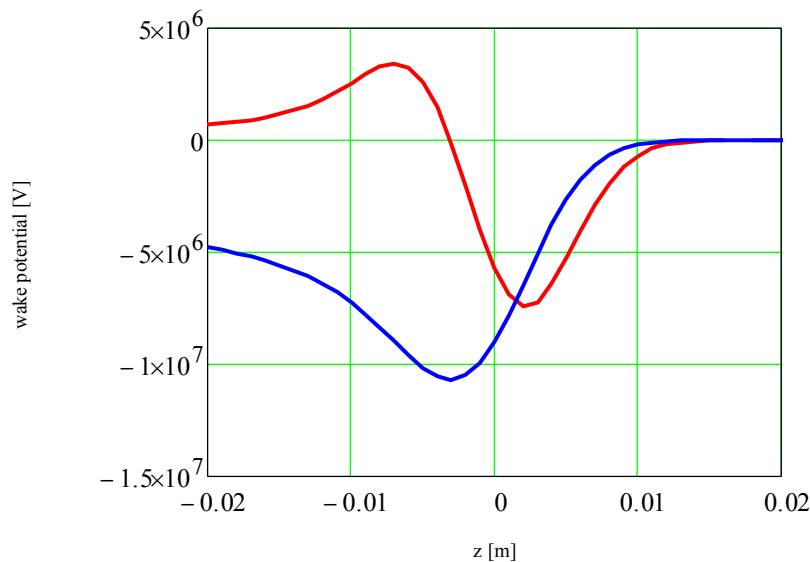
$$V(z) = \int_z^{\infty} dz' \rho(z') W_{\parallel}(z-z')$$

$$\Delta E = eq \int_{-\infty}^{\infty} dz \rho(z) V(z)$$

$$W(z) = -\frac{16}{b^2} \left[\frac{1}{3} \exp\left(\frac{z}{s_0}\right) \cos\left(\frac{\sqrt{3}z}{s_0}\right) - \frac{\sqrt{2}}{\pi} \int_0^{\infty} dx \frac{x^2 \exp\left(\frac{x^2 z}{s_0}\right)}{x^6 + 8} \right]$$

$$s_0 = \left(\frac{2cb^2}{4\pi\sigma} \right)^{1/3}$$

Energy losses: 9.8 MeV
 Energy spread: 3.6 MeV

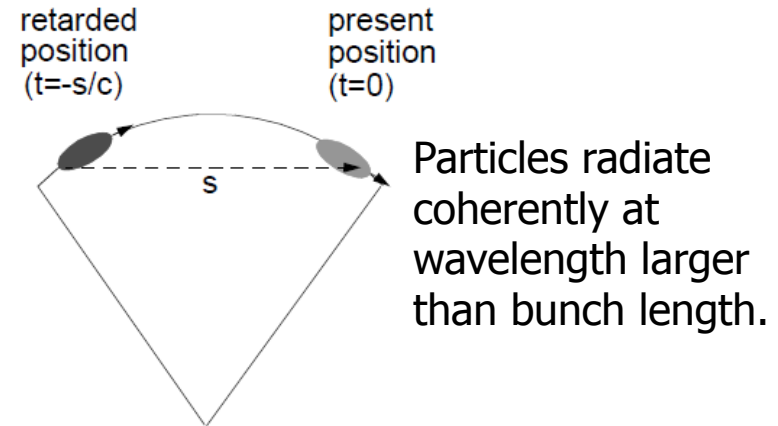


RW and **RF** contributions

Courtesy of A. Fedotov and W. Xu

CSR (estimate **without** taking into account beam pipe shielding effect)

$$\left(\frac{dE}{d(ct)} \right) = -\frac{2q^2}{3^{1/3} R^{2/3}} \int_{-\infty}^s \frac{ds'}{(s-s')^{1/3}} \frac{d\lambda(s')}{ds'}$$



For Gaussian distribution:

energy loss: $\langle E \rangle = -0.35 \frac{r_e N_e L_{eff}}{\gamma (R^2 \sigma_{es}^4)^{1/3}}$

energy spread: $\sigma_E = 0.25 \frac{r_e N_e L_{eff}}{\gamma (R^2 \sigma_{es}^4)^{1/3}}$

used parameters:

Bunch charge	5.3nC
Rms bunch length	4 mm
Vacuum chamber height	+/- 10 mm

For eRHIC, without shielding by vacuum chamber, effect would be significant.

CSR Suppression by Shielding from Beam Pipe

Effectiveness of shielding is described by parameter: $x_{th} = \frac{2\pi^3 R \sigma_z^2}{3h^3}$

- For $x < 1$, there is no suppression from shielding.
- For $1 < x < 4\pi^2$, there is strong reduction of CSR: $F(x) = x^{-1/3} e^{-x}$
- For $x > 4\pi^2$, CSR power is completely suppressed by shielding: $\sigma_{th,min} = \sqrt{\frac{6h^3}{\pi R}}$
- For eRHIC, full suppression of CSR for 4mm rms bunch length and $h=2$ cm full gap size requires $R > 1\text{m}$: $x_{th}=4\pi^2$

Examples of analytic treatment of shielding: Schwinger' 45; impedance: Warnock' 90 [1]; wake function: Murphy-Krinsky-Gluckstern' 96; Agoh-Yokoya' 94 [2]; Mayes-Hoffstaetter' 09 [3].

Suppression factor

For eRHIC parameters:
 $> 10^{17}$ for $R > 1\text{m}$

Courtesy of A. Fedotov

PRL **109**, 164802 (2012)

PHYSICAL REVIEW LETTERS

week ending
19 OCTOBER 2012

Experimental Observation of Suppression of Coherent-Synchrotron-Radiation-Induced Beam-Energy Spread with Shielding Plates

V. Yakimenko,¹ M. Fedurin,¹ V. Litvinenko,^{1,2} A. Fedotov,¹ D. Kayran,¹ and P. Muggli³

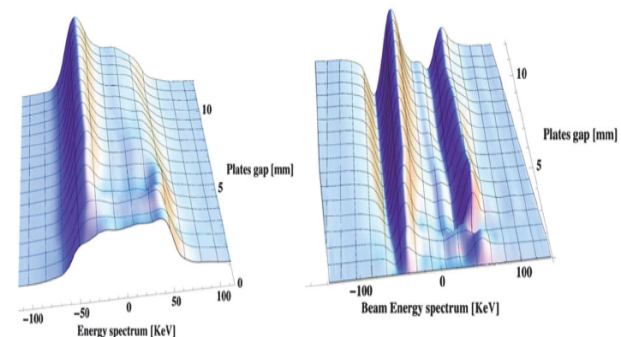
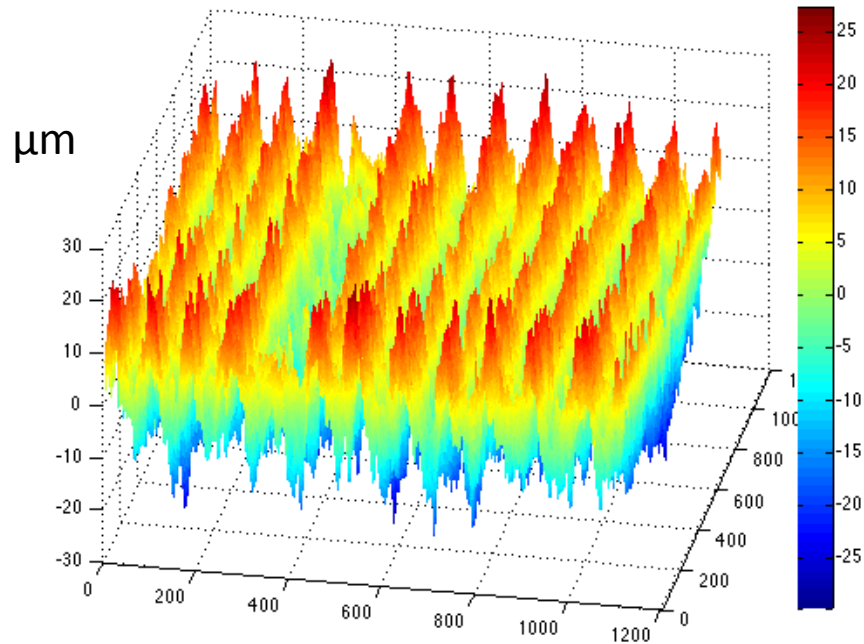


FIG. 3 (color). Measured beam-energy spectra as function of the gap between the shielding plates (on the left). The charge displacement map calculated from this result by subtracting the energy spectrum obtained with the plate gap of 1 mm from the other spectra is shown on the right.

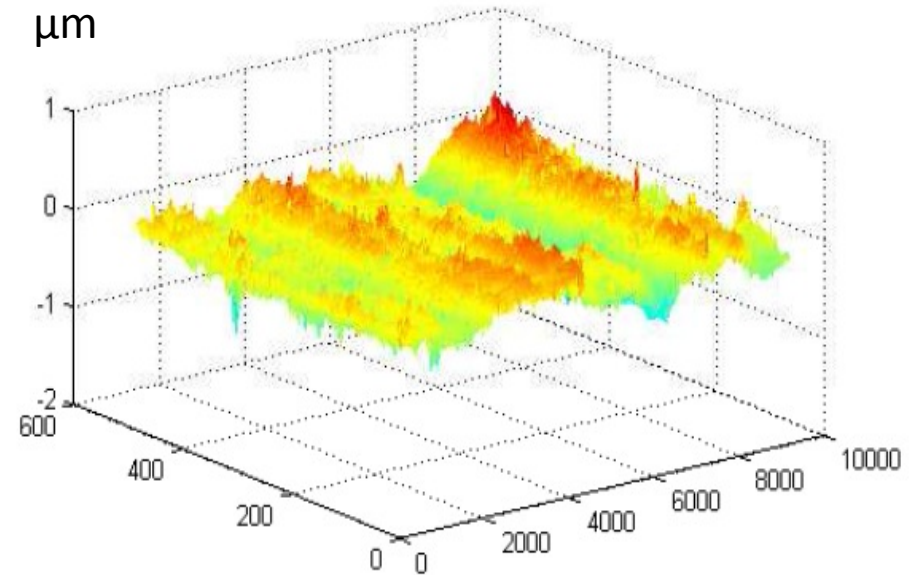
Energy Spread and Energy Losses due to Wall Roughness: Measured surface:



“surface-1”. extruded aluminum from the NSLS-II vacuum chamber. Extrusions are along the mountain ridges (red).

Measurements are courtesy of P. Takacs of the Instrumentation Division of BNL.

Courtesy of A. Fedotov



“surface-2”: from the vacuum chamber for superconducting undulator. Extrusions were done by "Cardinal Aluminum" at Louisville, KY.

The sample beam pipe was provided by Emil Trakhtenberg (ANL).

eRHIC WR estimates

- Using factors obtained from NOVO simulations (conservative): 24

For eRHIC present parameters with bunch length 4 mm and half-gap 1 cm :

Even NSLS-II surface is reasonable:

DE= 3.8 MeV (after all passes)

Using reduction factor from “ANL surface”:

DE=+/- 0.1 MeV (after all passes)

Summary: for the same surface as extruded aluminum small-gap chambers from ANL (rms height of roughness $d=0.2$ microns), effect of WR is negligible.

For present eRHIC parameters requirements on d can be relaxed to about 1-2 microns rms.

Summary for Energy Losses and Energy Spread Due to the Considered Effects

- The energy losses and energy spread due to CSR is expected to be completely suppressed by the shielding from the beam pipe.
- The wake field due to wall roughness causes 3.7 MeV energy spread with the NSLS-II beam pipe, which can be improved to 0.1 MeV level by improving extrusion aperture surface finish.
- The major contribution of energy losses and energy spread so far comes from the wake field of **the resistive wall and the srf cavities**. **The total energy losses is 9.8 MeV and the full energy spread is +/- 7.4 MeV.**

bunch charge	5.3nC
rms bunch length	4 mm
vacuum chamber full height	20 mm

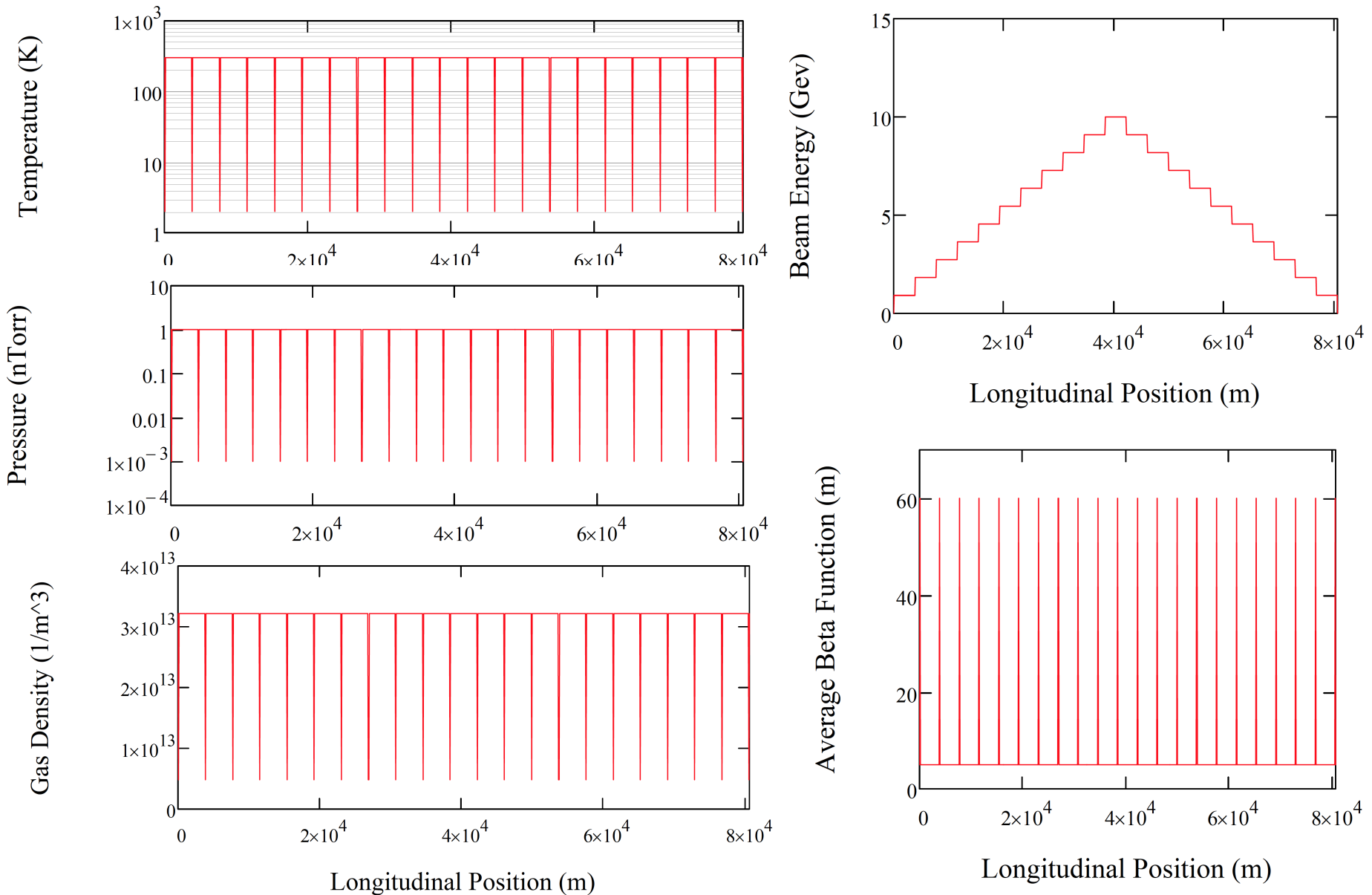
	Energy loss [MeV]	Rms energy spread [MeV]	Power loss [MW]
CSR	suppressed	suppressed	
Resistive wall	3.4	3.5	0.17
Cavities	6.4	3.0	0.32
Wall roughness	negligible	negligible	
Synch. radiation	25.7	0.49	1.28
Total	35.5	3.6*	1.78

Courtesy of A. Fedotov

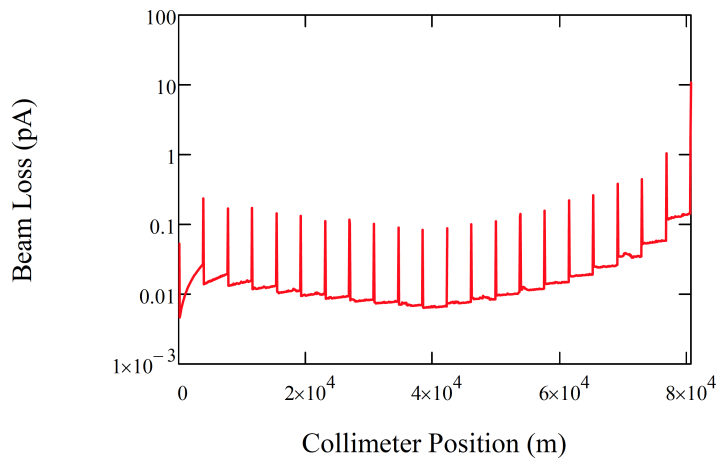
* The full energy spread is +/- 7.4 MeV.

Beam Losses Due to Gas Scattering:

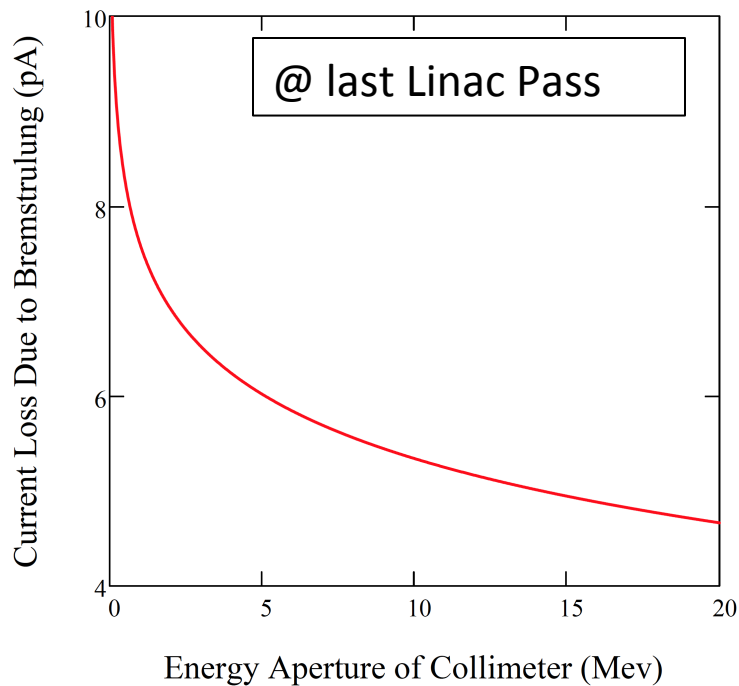
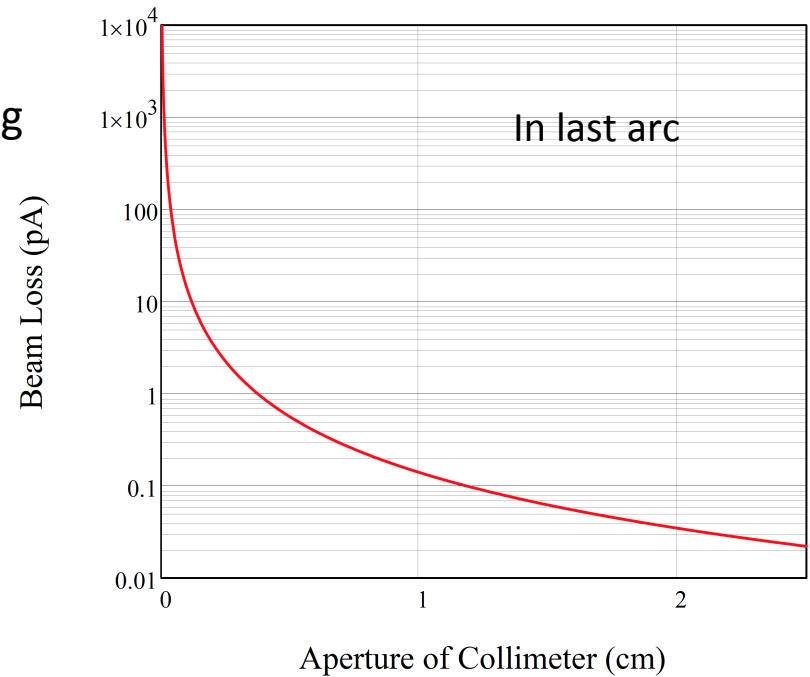
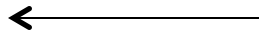
Lattice Parameters



Beam Losses Due to Elastic Scattering and Bremsstrahlung

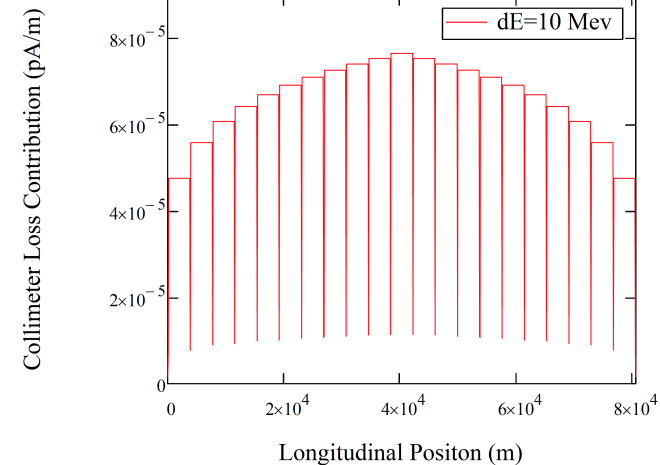


Elastic scattering

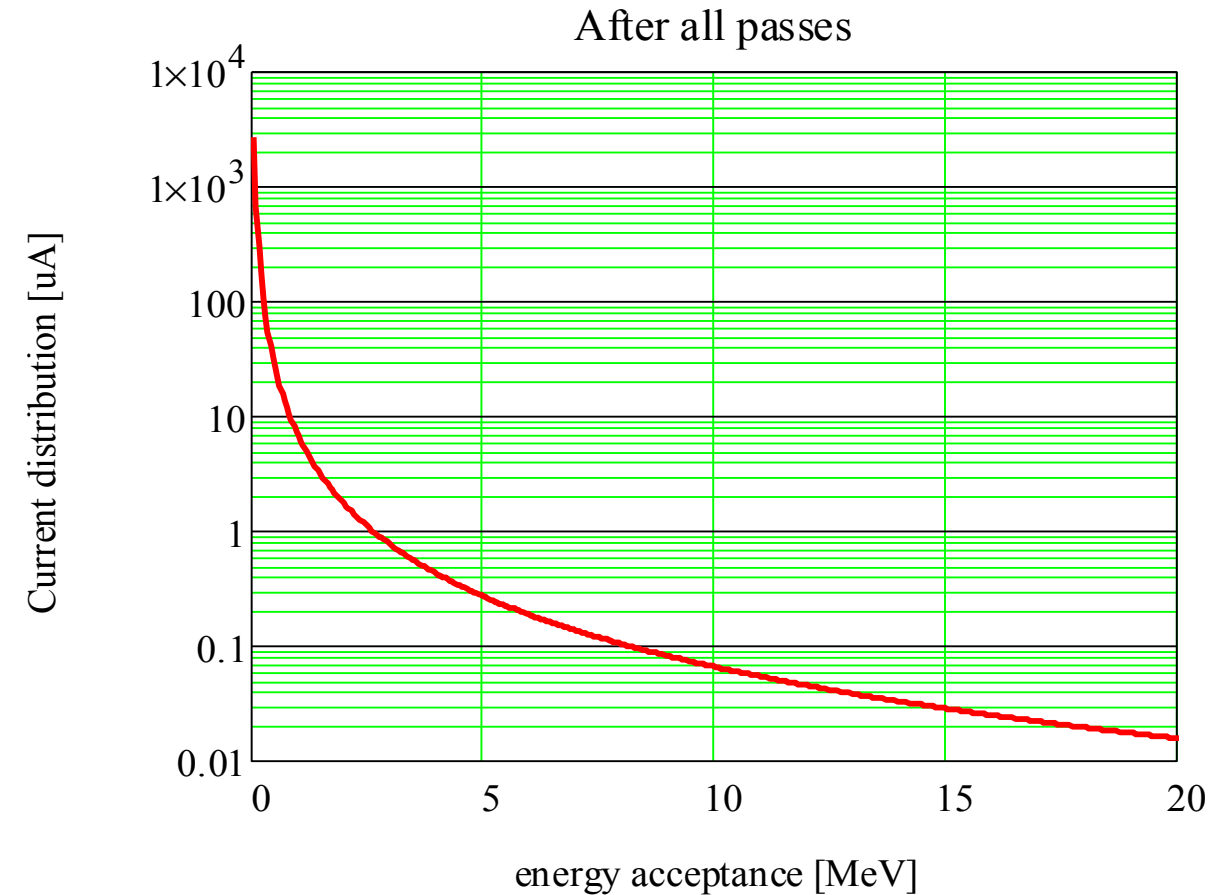


Bremsstrahlung

The location of collimators will be optimized to low energy passes to minimize power losses.



Beam Losses due to Touschek Effects



Parameters	
I_{avg}	50 mA
ϵ_n	20 μm
σ_z	4 mm

Courtesy of A. Fedotov

Summary for Beam Losses Due to Touschek Effect and Scattering with Residue Gas

- **Touschek effect** is currently the dominant mechanism for beam losses. **Depending on energy acceptance, beam losses ranges from 15 ~ 300 nA (20MeV~5MeV).**
- Depending on transverse aperture, beam losses due to elastic scattering varies from 0.15~0.6 pA (1cm~5mm) under the present model. Depending on energy deviation aperture, beam loss due to bremsstrahlung varies from 4.6~7.6 pA (20Mev~1Mev).

Summary

- For the considered collective effects, **we do not see any show-stoppers so far from our current studies.**
- We have **a long to-do list to improve** these estimations and our understandings of the collective effects for the FFAG-based eRHIC.
 - simulate with real lattices for FII
 - connect all energy passes for FII
 - simulate with realistic gas species for FII
 - effects from beams with different energies for FII
 - chromatic dephasing effects to Multi-bunch BBU
 - Horizontal single bunch BBU due to resistive wall wake
 - Landau damping in single bunch BBU
 - ...

Thank you!

Equation of motion

$$\frac{d}{dt} p_x(z, s) = m_e c^2 \left\{ \beta(s)^2 \frac{d}{ds} \left[\gamma(s) \frac{d}{ds} x(z, s) \right] + \frac{1}{\gamma(s)^2} \left(\frac{d}{ds} x(z, s) \right) \cdot \left(\frac{d}{ds} \gamma(s) \right) \right\} = F_{focus}(z, s) + F_{wake}(z, s)$$

$$F_{focus}(z, s) = -m_e \beta(s)^2 c^2 \left(\frac{2\pi}{\lambda_x(z, s)} \right)^2 \gamma(s) x(z, s)$$

$$F_{wake}(z, s) = -e^2 \int_z^\infty dz' \rho(z') W_1(z' - z) x(z', s')$$



$$\gamma(s) \gg 1$$

$$\frac{d}{ds} \left[\gamma(s) \frac{d}{ds} x(z, s) \right] + \left(\frac{2\pi}{\lambda_x(z, s)} \right)^2 \gamma(s) x(z, s) = \frac{-e^2}{m_e c^2} \int_z^\infty dz' \rho(z') W_1(z' - z) x(z', s')$$



$$\gamma(s) = \gamma_i (1 + \alpha s)$$

$$\frac{d^2}{ds^2} x(z, s) + \frac{\alpha}{1 + \alpha s} \frac{d}{ds} x(z, s) + \left(\frac{2\pi}{\lambda_x(z, s)} \right)^2 x(z, s) = \frac{-e^2}{m_e c^2 \gamma_i (1 + \alpha s)} \int_z^\infty dz' \rho(z') W_1(z' - z) x(z', s')$$

In Arcs $\alpha = 0$

$$\frac{d^2}{ds^2} x(z, s) + \left(\frac{2\pi}{\lambda_x(z, s)} \right)^2 x(z, s) = \frac{-e^2}{m_e c^2 \gamma_i} \int_z^\infty dz' \rho(z') W_1(z' - z) x(z', s)$$

Consider wake field due to resistive wall: $W_1(z' - z) = -\frac{2}{4\pi^2 \epsilon_0 b^3} \sqrt{\frac{4\pi \epsilon_0 c}{\sigma z}} = -\frac{1}{\pi^{3/2} b^3} \sqrt{\frac{c}{\epsilon_0 \sigma z}}$

$$\boxed{\frac{d^2}{ds^2} x(z, s) + \left(\frac{2\pi}{\lambda_x(s)} \right)^2 x(z, s) = \frac{1}{\pi^{3/2} b^3} \frac{e^2}{m_e c^2 \gamma_i} \int_z^\infty dz' \rho(z') \sqrt{\frac{c}{\epsilon_0 \sigma (z' - z)}} x(z', s)} \quad (1)$$

Follow iterative/perturbative method to solve (1)

First step
$$\frac{d^2}{ds^2} x^{(0)}(z, s) + k_0^2 x^{(0)}(z, s) = 0$$

Then
$$\frac{d^2}{ds^2} x^{(n)}(z, s) + k_0^2 x^{(n)}(z, s) = \frac{1}{\pi^{3/2} b^3} \frac{e^2}{m_e c^2 \gamma_i} \int_z^\infty dz' \rho(z') \sqrt{\frac{c}{\epsilon_0 \sigma (z' - z)}} x^{(n-1)}(z', s)$$

$$x(z, s) = \sum_{n=0}^{\infty} x^{(n)}(z, s)$$

Conditions for this to work $|x^{(n)}| \ll |x^{(n-1)}|$, i.e. the sum has to converge fast enough.

Elastic Scattering

Cross Section and Angle Aperture

$$\sigma(\theta) = \int_{\theta}^{\theta_{\max}} \left(\frac{d\sigma}{d\Omega} \right)_{\theta < 1} d\Omega = 4\pi Z_i^2 r_e^2 \left(\frac{m_e c}{\beta p} \right)^2 \left[\frac{1}{\theta^2 + \theta_{\min}^2} - \frac{1}{\theta_{\max}^2 + \theta_{\min}^2} \right]$$

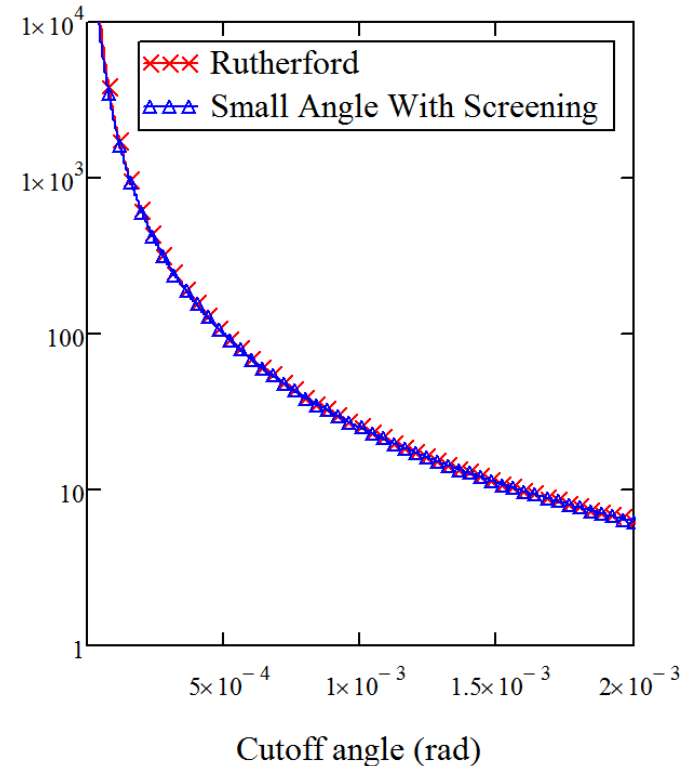
Angle Aperture Due To Collimeter at
Certain Location

$$\theta(z_{scatter}) > \frac{y_{coll}}{\sqrt{\beta_{scatter} \beta_{coll}} \sin \Delta\psi} \sqrt{\frac{E_{coll}}{E_{scatter}}}$$

Averaging over initial phases for all particles

$$\theta(z_{scatter}) > \frac{2y_{coll}}{\sqrt{\beta(z_{scatter}) \beta(z_{coll})}} \sqrt{\frac{E(z_{coll})}{E(z_{scatter})}}$$

Integrated Cross Section (barn)



(Reference: P. Tenenbaum, LCC-NOTE-0051(2001))

Cross Section For Bremsstrahlung

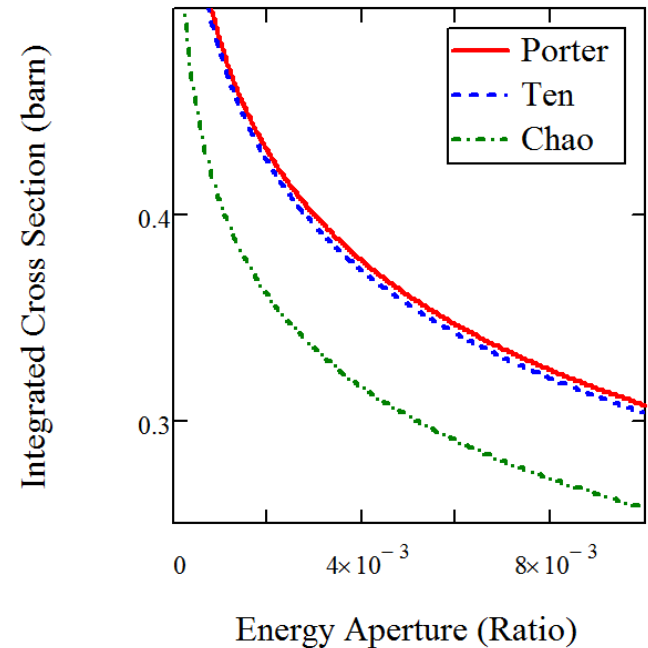
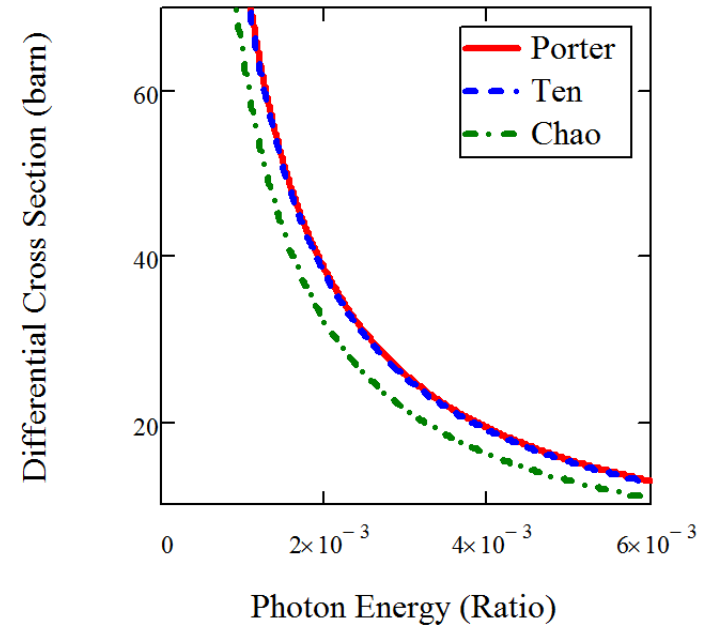
$$\left(\frac{d\sigma_{brem}}{dy} \right)_{Porter} = \frac{4\alpha_e^2}{y} \left\{ \left(\frac{4}{3} - \frac{4}{3}y + y^2 \right) \left[Z^2 (L_{rad} - f(\alpha^2 Z^2)) + ZL'_{rad} \right] + (1-y)(Z^2 + Z)/9 \right\}$$

$$y = \frac{E_{photon}}{E_{electron}} \quad L_{rad} = \ln\left(\frac{184.15}{Z^{1/3}}\right) \quad L'_{rad} = \ln\left(\frac{1194}{Z^{1/3}}\right) \quad f(x) = x \sum_{n=1}^{\infty} \frac{1}{n(n^2 + x)}$$

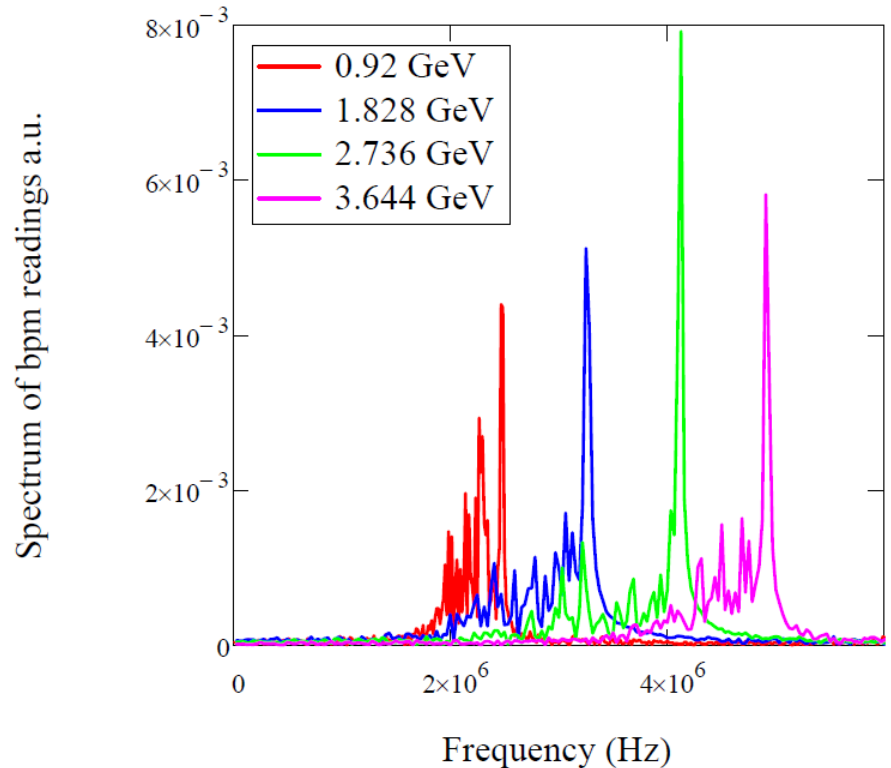
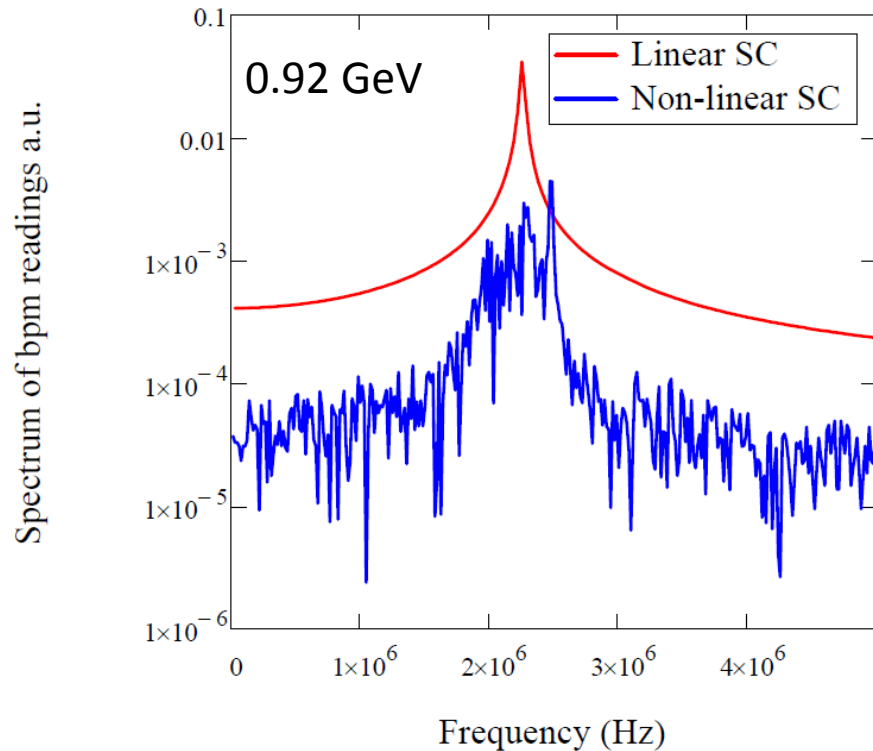
$$\begin{aligned} & (\sigma_{brem}(u_{min}))_{Porter} \\ &= \int_{u_{min}}^1 \left(\frac{d\sigma_{brem}}{dy} \right)_{Porter} dy \\ &= \frac{16\alpha_e^2}{3} \left\{ \left(-\ln(u_{min}) - \frac{5}{8} + u_{min} - \frac{3}{8}u_{min}^2 \right) \left[Z^2 (L_{rad} - f(\alpha^2 Z^2)) + ZL'_{rad} \right] \right. \\ & \quad \left. - \frac{(Z+1)(\ln(u_{min}) + 1 - u_{min})}{12} \right\} \end{aligned}$$

Reference:

1. 'Handbook of Accelerator Physics and Engineering' by A.W.Chao p.213
2. 'Beam-Gas and Thermal Photon Scattering in the NLC Main Linac as a Source of Beam Halo' by P. Tenenbaum, LCC-NOTE-0051(2001)
3. 'Luminosity lifetime at an asymmetric e+e- collider' NIM A302 (1991) 209-216, by F.C.Porter

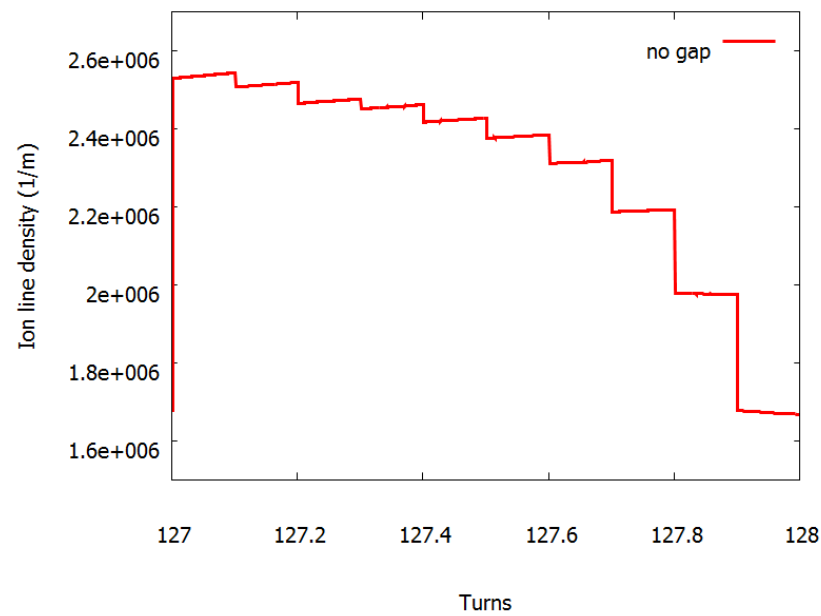
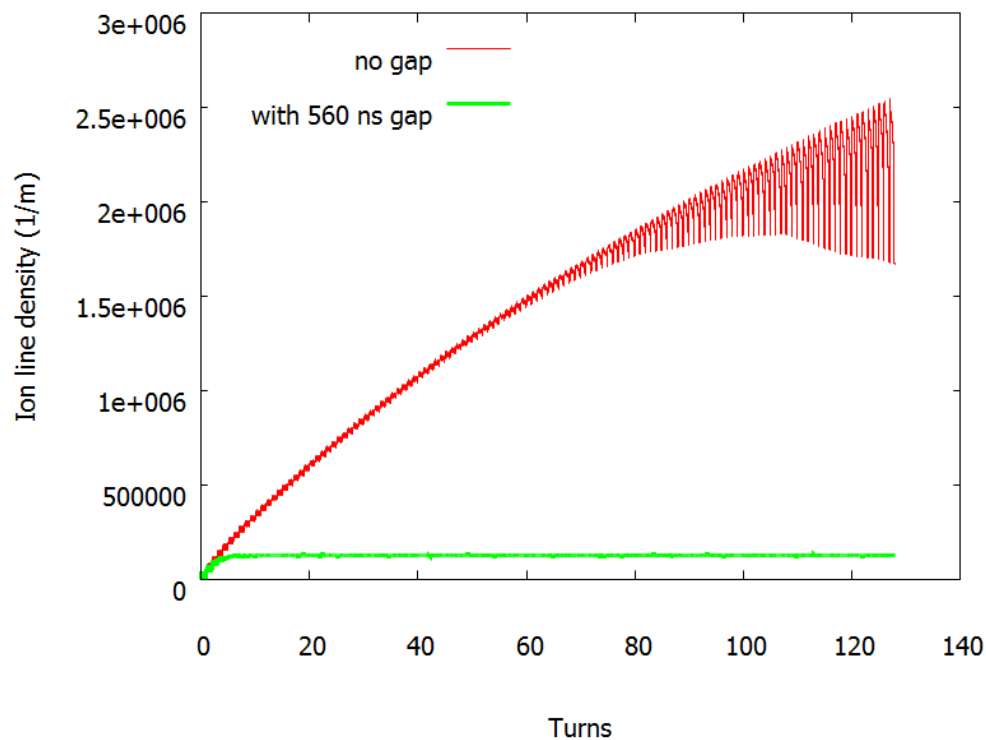


FII: Spectrum of Bpm Data



- The spectra of the bpm data from different energy passes do overlap due to non-linear space charge frequency shift. Simulations following the beam for all 20 passes is needed.

Evolution of Ion Line Density



Equation of Motion

(No Landau Damping, T.O. Raubenheimer and F. Zimmermann PRE 52, P. 5487-5498, (1995))

Assumptions for linear model to work: $y_b, y_i < \sigma_{x,y}$

$$\frac{d^2 \tilde{y}_i(s, t)}{dt^2} + \omega_i^2 (ct - s) \tilde{y}_i(s, t) = \omega_i^2 (ct - s) y_b(s, ct - s) \quad \text{Beam driving ion oscillation}$$

$$\frac{d^2 y_b(s, z)}{ds^2} + \omega_\beta^2 y_b(s, z) = K [y_i(s, s + z) - y_b(s, z)] \int_{-\infty}^z \rho(z') dz'$$

$$y_i(s, t) = \frac{\int_{-\infty}^z \rho(z') \tilde{y}_i(s, t | s + z') dz'}{\int_{-\infty}^z \rho(z') dz'}$$

Beam is modulated by the oscillation of ions' centroid

Ions generated at different time work together according to superposition principal.

$$K(n_b) = \frac{2N_e n_b d_{gas} \sigma_{ionization} r_e}{\gamma_e \Sigma_y (\Sigma_y + \Sigma_x)} \approx \frac{4N_e n_b d_{gas} \sigma_{ionization} r_e}{3\gamma_e \sigma_y (\sigma_y + \sigma_x)}$$

Coupling strength of ions after a train of nb bunches passing by. **The density of neutral gas is constant during the process.**

$$\omega_i = \left[\frac{4N_e r_p}{3L_{sep} \sigma_y (\sigma_x + \sigma_y) A} \right]^{1/2} c$$

Ion oscillation frequency, **smooth focusing approximation.**

Solution

- Assumptions used in finding solutions:

$$\omega_\beta s \gg 1 \quad \omega_i z_0 \gg 1 \quad \rho(z) = \begin{cases} \frac{1}{2z_0} & \text{for } |z| < z_0 \\ 0 & , \text{ otherwise} \end{cases}$$
- Initial condition (Fourier component of shot noise at ion's characteristic oscillation frequency):

$$y_b(0, z) = \hat{y} \sin(\omega_i z + \theta)$$

- Assuming $K / \omega_\beta \ll 1$ and following a perturbative method, they obtain:

$$\eta(s, z) \equiv \frac{K \omega_i (z + z_0)^2 s}{16 z_0 \omega_\beta} = \frac{N_e^{3/2} d_{\text{gas}} \sigma_{\text{ionization}} r_e r_p^{1/2} \beta_x (z + z_0)^2 s}{3^{3/2} \gamma_e \sigma_y^{3/2} L_{\text{sep}}^{3/2} (\sigma_y + \sigma_x)^{3/2} A^{1/2}}$$

$$y_b(s, z) = \frac{\hat{y}}{2} \left\{ J_0 \left[2\sqrt{\eta(s, z)} \right] \sin(\omega_i z + \omega_\beta s + \phi + \theta) + \right. \\ \left. + I_0 \left[2\sqrt{\eta(s, z)} \right] \sin(\omega_i z - \omega_\beta s - \phi + \theta) \right\}$$

Asymptotic Growth Time

The amplitude of the growing term behaves as

$$I_0 \left[2\sqrt{\eta(s,z)} \right] \approx \frac{1}{\sqrt{4\pi}} \frac{e^{2\sqrt{\eta(s,z)}}}{\eta(s,z)^{1/4}} = \sqrt{\frac{\tau_{grow}}{2\pi t}} e^{t/\tau_{grow}} \quad \text{for } t \gg \tau_{grow}$$

$$\eta(s,z) \equiv \frac{K\omega_i (z+z_0)^2 s}{16z_0\omega_\beta} = \frac{N_e^{3/2} d_{gas} \sigma_{ionization} r_e r_p^{1/2} \beta_x (z+z_0)^2 s}{3^{3/2} \gamma_e \sigma_y^{3/2} L_{sep}^{3/2} (\sigma_y + \sigma_x)^{3/2} A^{1/2}}$$

Observing at a given location, s , the displacement of incoming bunches grows exponentially with a growth time of

$$\frac{t}{\tau_{grow}} = 2\sqrt{\eta(s,z)}$$

$$\Rightarrow \tau_{grow} = \sqrt{\frac{(z+z_0)^2}{4c^2 \eta(s,z)}} = \sqrt{\frac{3^{3/2} \gamma_e L_{sep}^{3/2} \sigma_y^{3/2} (\sigma_y + \sigma_x)^{3/2} A^{1/2}}{4c^2 N_e^{3/2} d_{gas} \sigma_{ionization} r_e r_p^{1/2} \beta_x s_{obs}}}$$

Results II: how far it can grow exponentially?

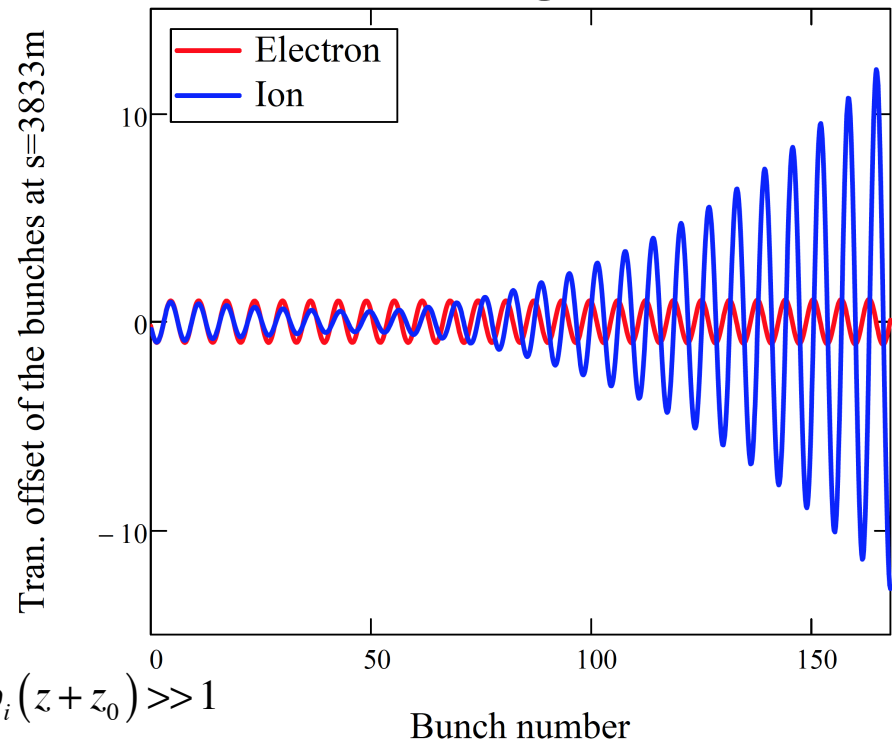
- From linear theory, ions will oscillate with greater amplitude before substantial electron oscillation develops.
- The linear theory breaks when the separation of the centroids of the ions and the electrons become larger than the electron beam size.
- Hence, it is likely that the fast growth predicted by linear theory will saturate at $y_b \ll \sigma_y$

$$y_i(s, s+z) \approx y_b(s, z)$$

$$-\frac{\hat{y}\omega_i(z+z_0)}{8\sqrt{\eta}} \left\{ I_1(2\sqrt{\eta}) \cos(\omega_i z + \theta - \omega_\beta s - \phi) + J_1(2\sqrt{\eta}) \cos(\omega_i z + \theta + \omega_\beta s + \phi) \right\}$$

$$y_i / y_b \sim \omega_i(z+z_0) / (4\sqrt{\eta}) = 53.3 \quad \text{for } \omega_\beta s \gg 1 \quad \text{and} \quad \omega_i(z+z_0) \gg 1$$

$$y_b / \sigma_y \sim 2\% \quad \text{for 1.9 GeV energy pass}$$

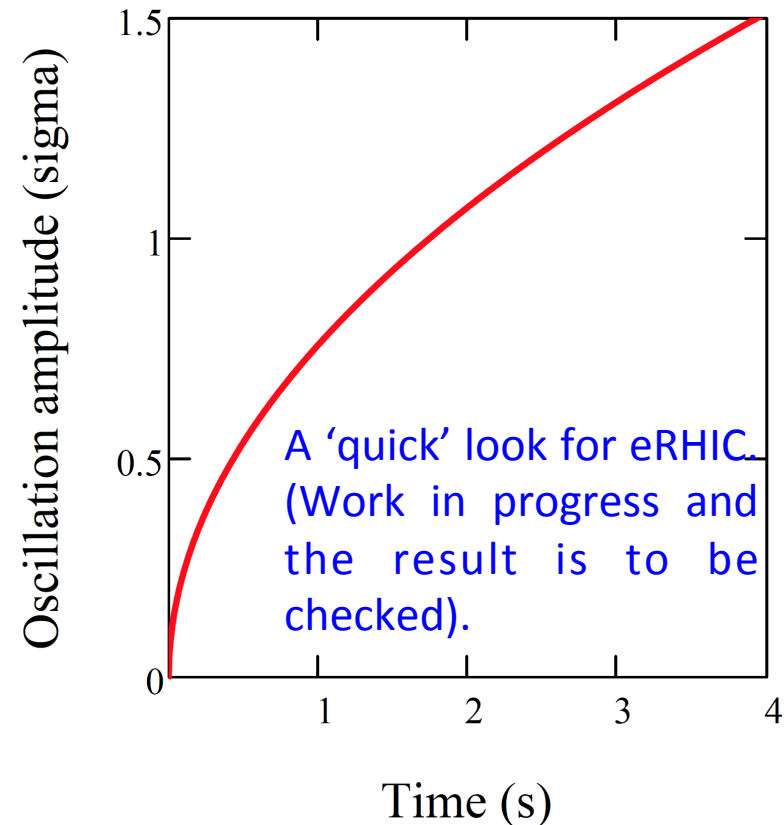
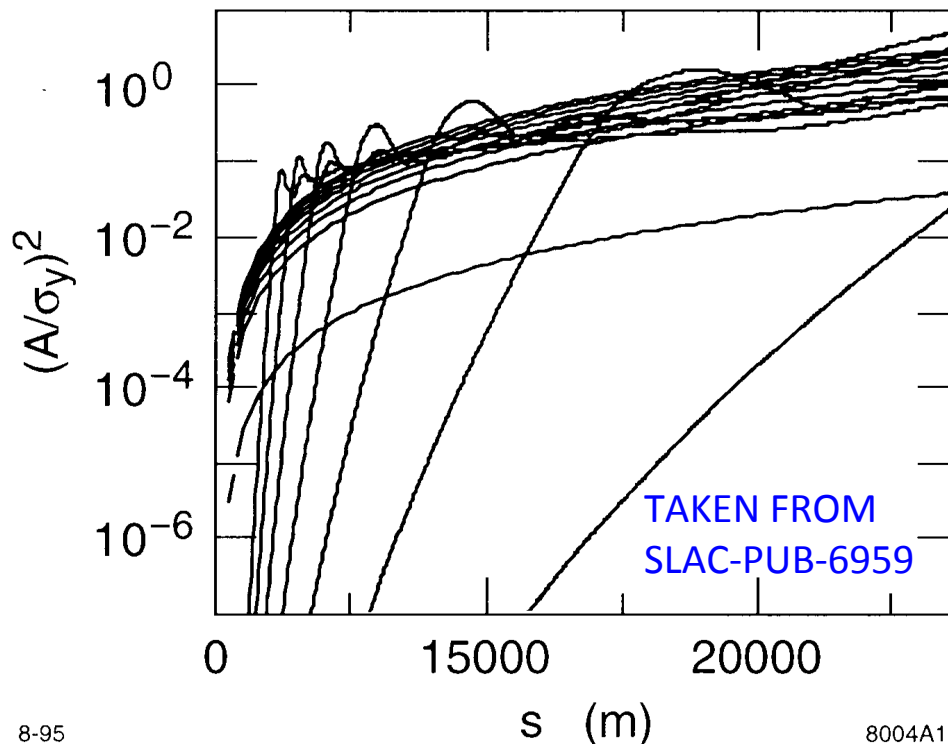


What happens after exponential growth?

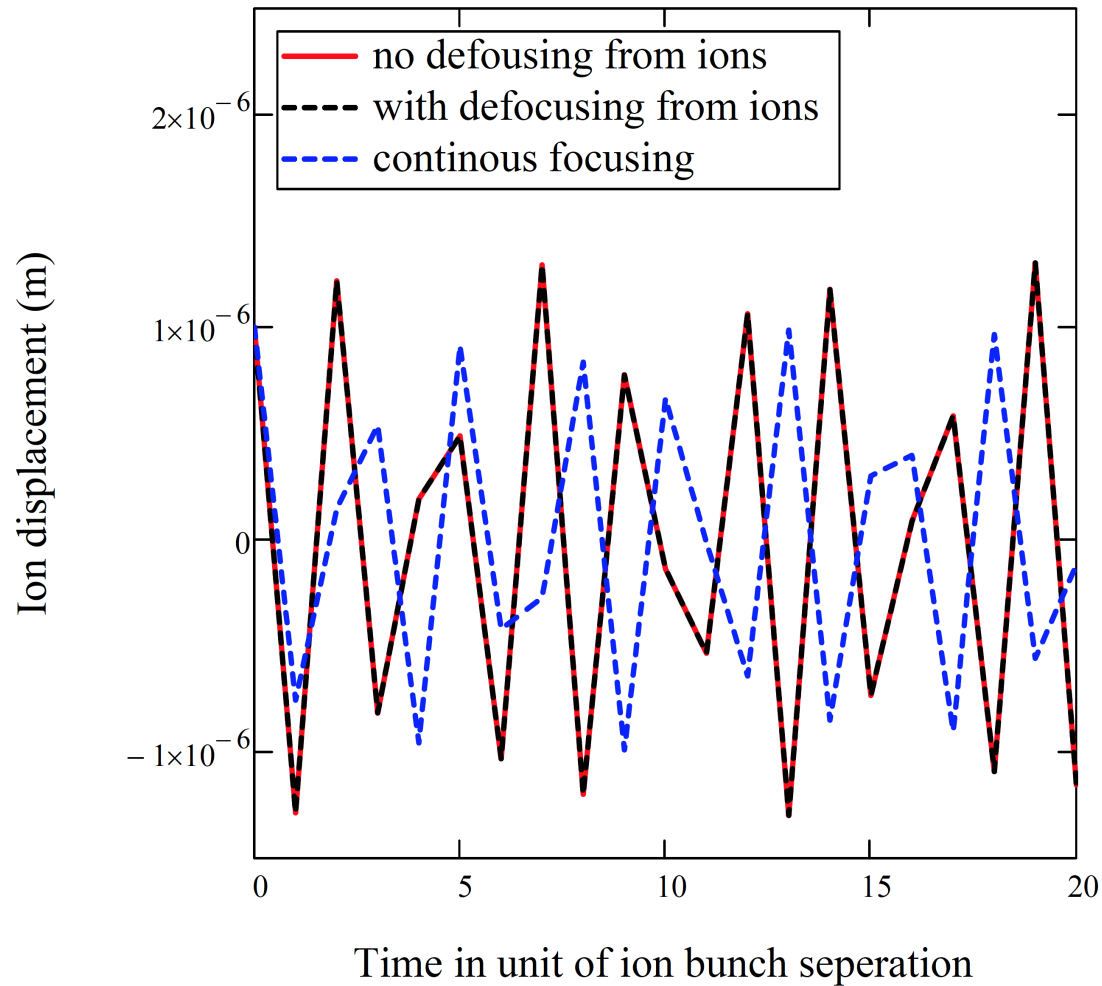
(Reference: S. A. Heifets, SLAC-PUB-6959)

WORK IN PROGRESS.....

$$\left\langle \left[\frac{y_b(s, z_n)}{\sigma_y} \right]^2 \right\rangle \simeq \left(\frac{s}{s_{eff}} \right)^2 (\omega_y s_b)^2 n. \quad \frac{1}{s_{eff}} = \frac{\kappa}{2\omega_b\omega_y}, \quad K = \kappa z_0$$

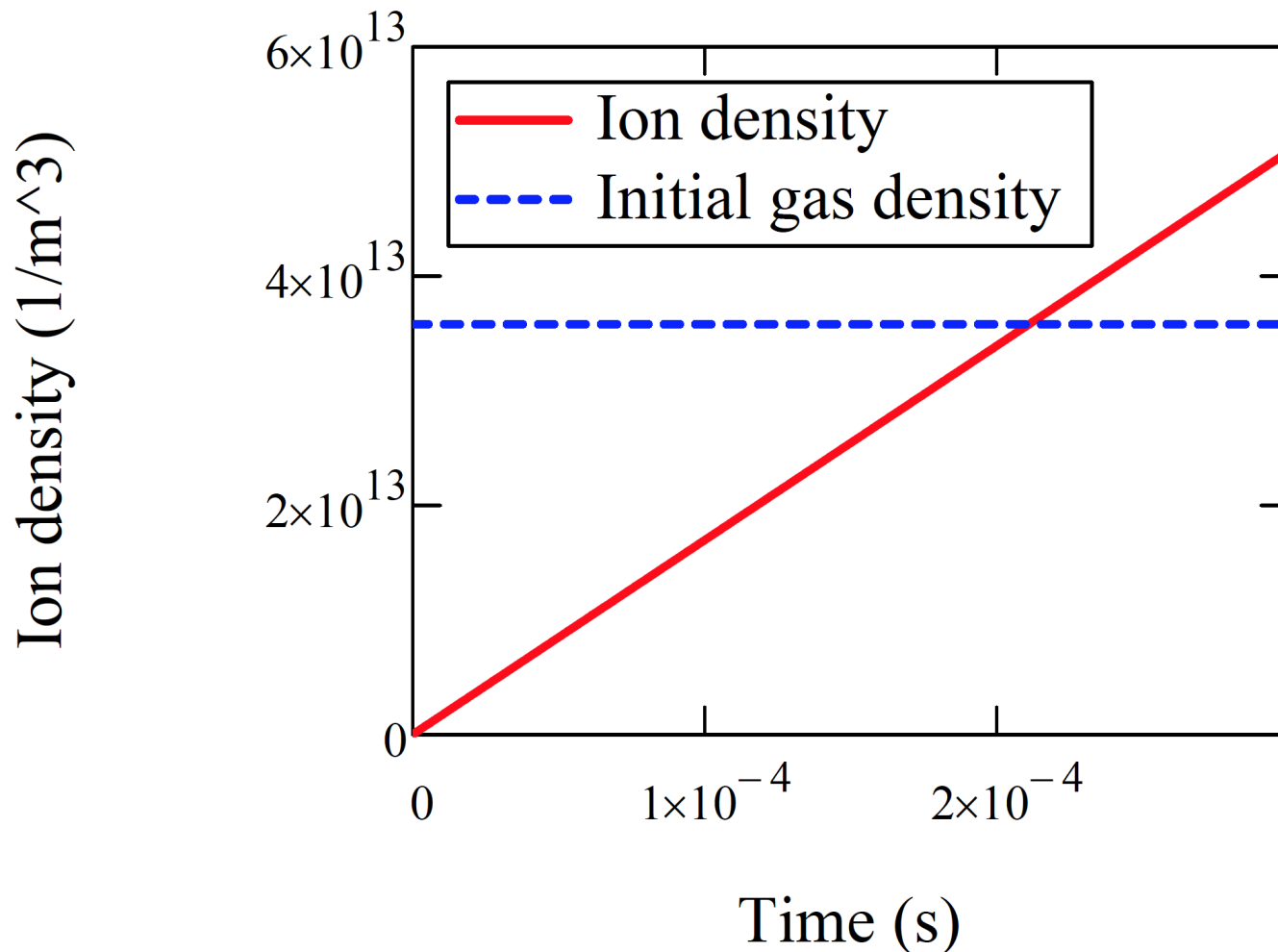


Checking Assumptions: validity of continous focusing

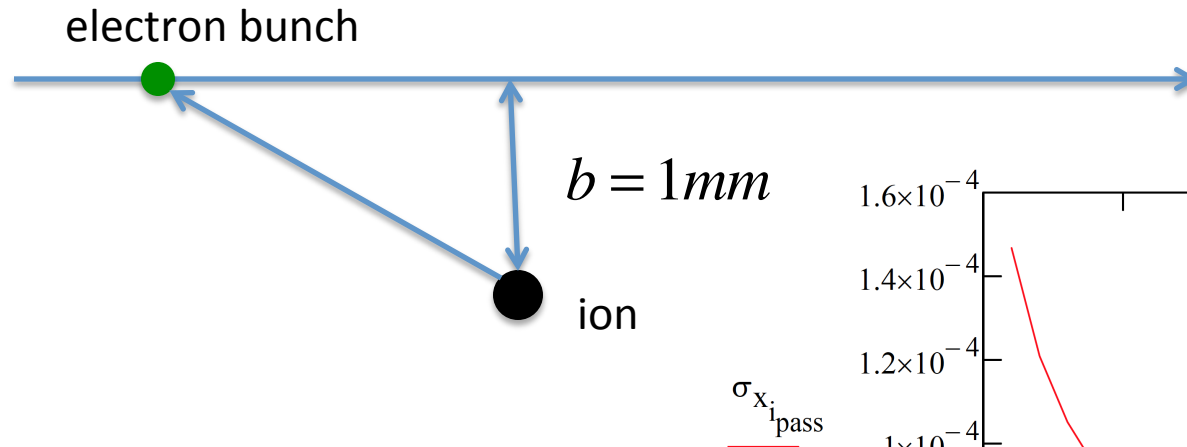


Checking Assumptions:

no saturation due to lacking gas molecule



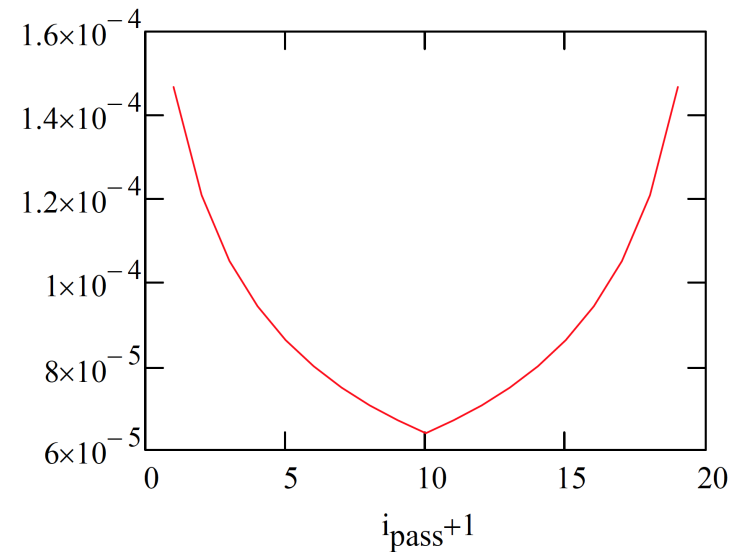
Checking Assumptions: effects from nearby bunches with other energies



$$F_x = \frac{\gamma Q_e e b}{4\pi\epsilon_0 \left[b^2 + (\gamma\beta ct)^2 \right]^{3/2}}$$

$$\Delta v_x = \frac{\Delta p_x}{m_p A_i} = \frac{\gamma Q_e e b}{4\pi\epsilon_0 m_p A_i} \int_{-\infty}^{\infty} \frac{dt}{\left[b^2 + (\gamma\beta ct)^2 \right]^{3/2}} = \frac{Q_e e}{2\pi\epsilon_0 m_p A_i \beta b c}$$

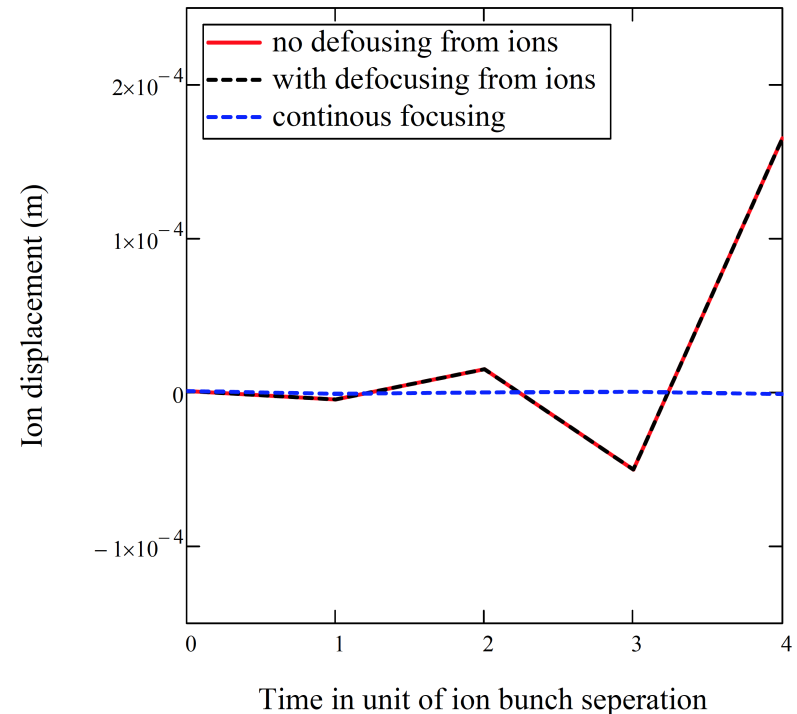
$$\Delta x = \Delta v_x \frac{L_{\text{sep}}}{c} = 63.5\mu\text{m}$$



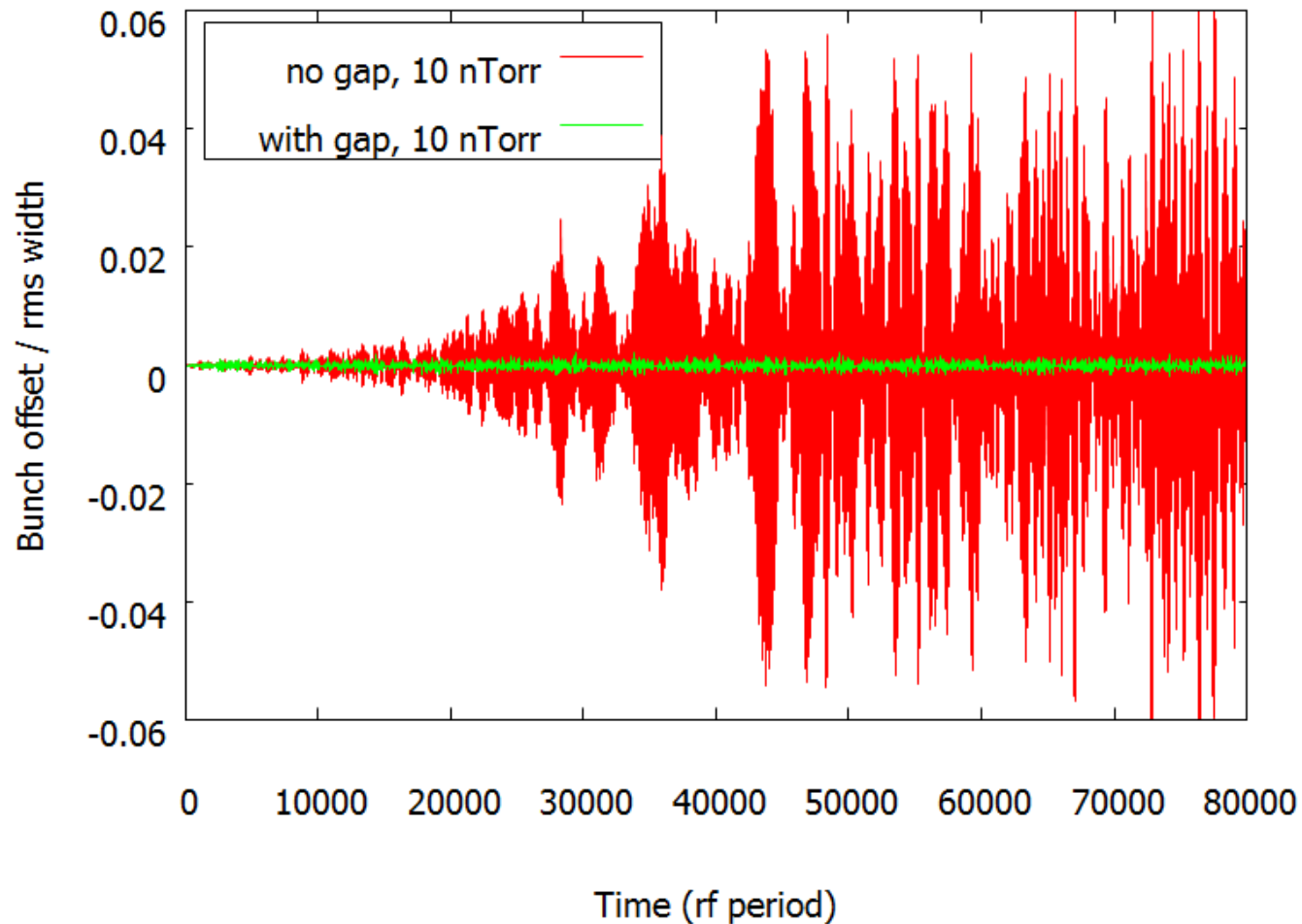
One Possible Way to Avoid The Instability: Over Focusing

$$A_{crit} = \frac{N_e r_p L_{sep} c}{2\sigma_x (\sigma_x + \sigma_y)} = \begin{cases} 10 & \text{if decelerating bunch is in the middle of two} \\ & \text{successive accelerating bunches;} \\ 41 & \text{if decelerating bunches overlap with accelerating} \\ & \text{bunches} \end{cases}$$

CO+ is overfocused by putting the accelerating bunch and the decelerating bunch 3/2 electron rf buckets away. The ions move out of the beam after seeing a few electron bunches.



Constant Neutral Gas Pressure: 10 nTorr (fast replenishment from surrounding gas molecules)



Wall Roughness (WR) Models

48

1. Bane et al. ('97) (also with Stupakov '98) **“The inductive”** model – small bumps of various shape. Contribution from a set of bumps is given by the sum of individual bump contributions to the impedance.

This is the model which was used to have quick “conservative” estimate for eRHIC in December 2010. Also used for LCLS design.

2. Stupakov ('98): “The Statistical” model
3. Novokhatski et al. ('97, '98, '99): **“The Resonator”** model

This model can lead not just to energy spread but also to energy loss due to propagation of synchronous modes.

4. M. Dohlus: ('00, '01) Impedance of corrugated pipe
5. Stupakov ('00): **“shallow”** corrugated pipe; surface impedance

Effect of beam pipe walls

49

One would expect the particles to radiate coherently at wavelengths comparable to the bunch length or larger.

However, the long-wavelength part of radiation spectrum will be strongly suppressed in the presence of shielding, for example conducting surfaces of the vacuum chamber.

This long-wavelength cutoff is not the usual wave-guide cutoff (comparable to the pipe diameter) but has a value that depends on the radius of the curvature as well as the pipe diameter -> typically, much smaller than the wave-guide cutoff. (simple physics picture: Heifets, Michailichenko' 91)

$$\frac{\pi}{h} < k\alpha = \omega\alpha / c = n\alpha / R < n^{2/3} / R$$

Hence, only harmonics with $n > (\pi R / h)^{3/2}$ can be emitted

accurate derivation gives: $n > n_{th} = \sqrt{\frac{3}{2}} (\pi R / h)^{3/2}$

(closed chamber evaluation gives n_{th} roughly equal to the one of parallel plates, Warnock' 90-91).

condition of coherence is then: $\frac{R}{\sigma_z} > n > \sqrt{\frac{3}{2}} (\pi R / h)^{3/2}$

Suppression of CSR by shielding

50

For radiation to be coherent the bunch length should be:

$$\sigma_z \leq \frac{h}{\pi} \sqrt{\frac{3h}{2\pi R}}$$

where h is beam pipe height, and
 R is the radius of the orbit in bending magnet.

$$\lambda_0 < \frac{\lambda}{2\pi} < \lambda_{th} \quad \text{If } l_{th} < l_0, \text{ CSR is strongly suppressed}$$

Shielding of CSR (analytic theories)

Examples of analytic treatment of shielding: Schwinger' 45; impedance: Warnock' 90 [1]; wake function: Murphy-Krinsky-Gluckstern' 96; Agoh-Yokoya' 94 [2]; Mayes-Hoffstaetter' 09 [3].

[1]:

$$\frac{Z(n, \omega)}{n} = \frac{2\pi^2 Z_0 R}{\beta} \sum_{p(\text{odd}) \geq 1} \Lambda_p \left[\frac{\beta \omega R}{nc} J'_n(\gamma_p R) ((J'_n(\gamma_p R) + iY'_n(\gamma_p R)) + \left(\frac{\alpha_p}{\gamma_p}\right)^2 J_n(\gamma_p R) (J_n(\gamma_p R) + iY_n(\gamma_p R)) \right],$$

[2]:

$$Z(\omega) = Z_0 \frac{2\pi}{h} \left(\frac{2c}{\omega \rho} \right)^{1/3} \sum_{p=0}^{\infty} \left\{ \text{Ai}'(\beta_p^2) (\text{Ai}'(\beta_p^2) - i\text{Bi}'(\beta_p^2)) + \beta_p^2 \text{Ai}(\beta_p^2) (\text{Ai}(\beta_p^2) - i\text{Bi}(\beta_p^2)) \right\}$$

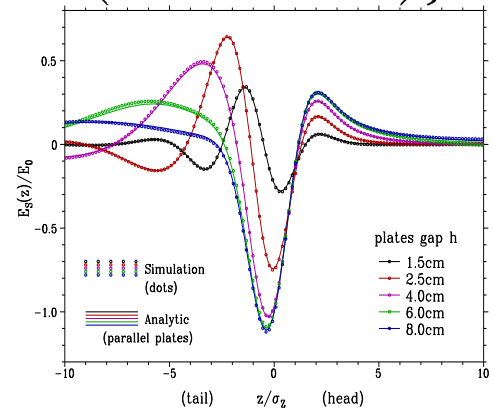
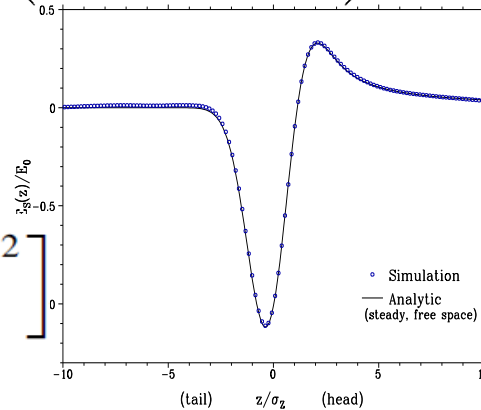
Asymptotic expression for impedance with shielding (strong shielding)

$$Z(k) = \frac{\pi Z_0}{kh^2} \left[e^{-2\pi^3 \rho / 3k^2 h^3} - \frac{3i}{2} C_5 \left(\frac{k^2 h^3}{\pi^3 \rho} \right)^2 \right]$$

$$\left. \frac{d\mathcal{E}_{\text{images}}}{ds}(s) \right|_B = Nr_c mc^2 \sum_{n=1}^{\infty} 2(-1)^n$$

[3]:

$$\times \left\{ \frac{-\kappa \lambda(s_{\alpha,n})}{r_{\alpha,n}} \right\}_{\alpha=-(\kappa L_m - \theta)}^{\alpha=\theta} + \int_{-(\kappa L_m - \theta)}^{\theta} d\alpha \frac{\beta^2 \cos(\alpha) - 1}{r_{\alpha,n}} \lambda'(s_{\alpha,n})$$



For eRHIC, full suppression of CSR for 4mm rms bunch length and h=2 cm full gap size requires $R > 1\text{m}$: $x_{\text{th}} = 4p^2$

$$x_{\text{th}} = \frac{2\pi^3 R \sigma_z^2}{3h^3}$$

CSR for eRHIC parameters

see also:

Suppression factor

For eRHIC parameters:
 $> 10^{17}$ for $R > 1\text{m}$

PRL **109**, 164802 (2012)

PHYSICAL REVIEW LETTERS

week ending
19 OCTOBER 2012

Experimental Observation of Suppression of Coherent-Synchrotron-Radiation-Induced Beam-Energy Spread with Shielding Plates

V. Yakimenko,¹ M. Fedurin,¹ V. Litvinenko,^{1,2} A. Fedotov,¹ D. Kayran,¹ and P. Muggli³

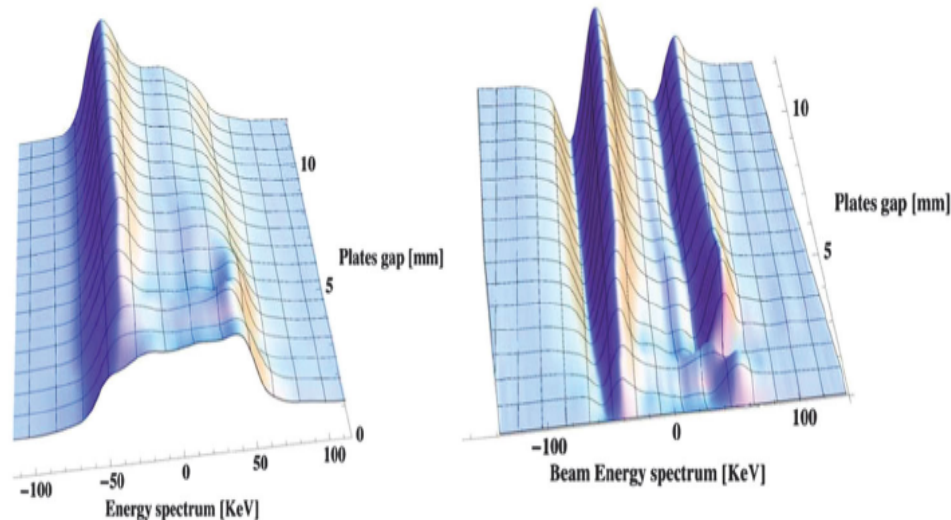
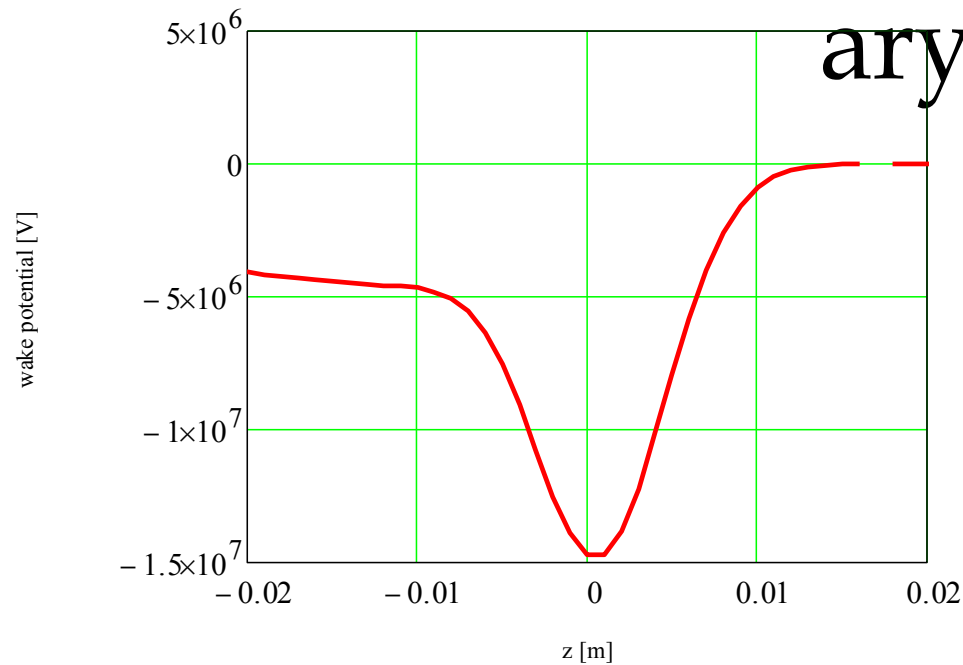


FIG. 3 (color). Measured beam-energy spectra as function of the gap between the shielding plates (on the left). The charge displacement map calculated from this result by subtracting the energy spectrum obtained with the plate gap of 1 mm from the other spectra is shown on the right.

Summary



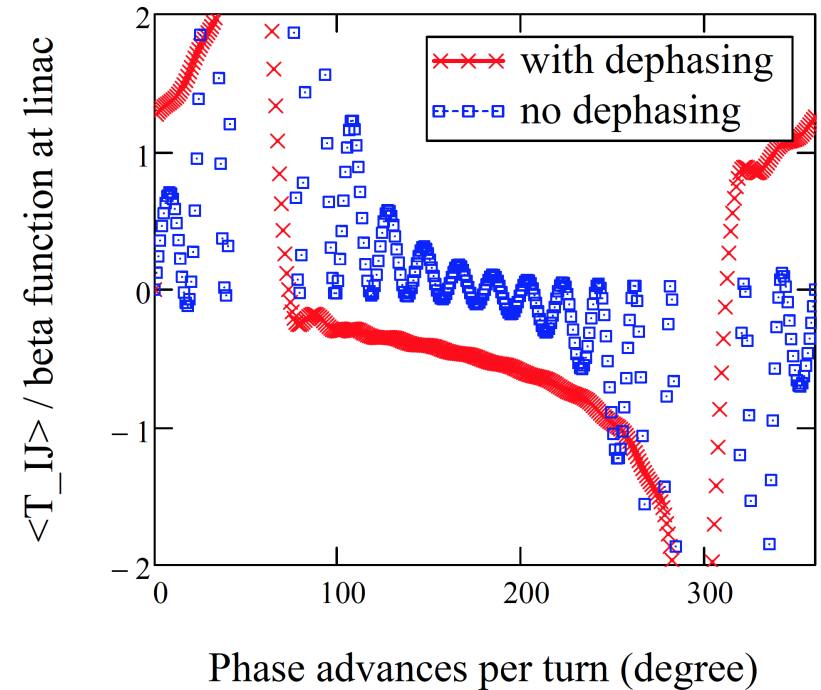
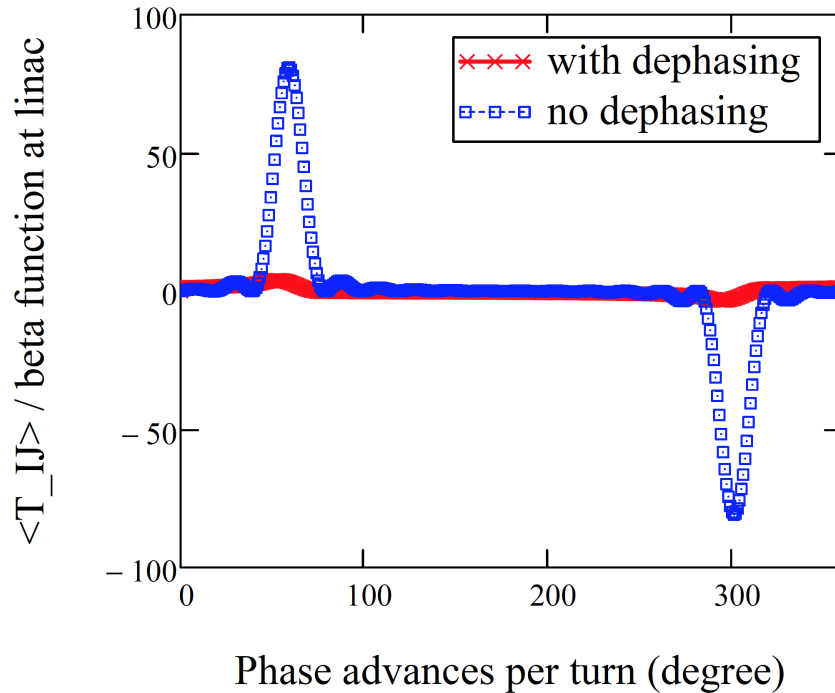
- Wake potential is dominated by RW and RF cavities.

Total: RW+WR (10 GeV)	Energy loss [MeV]	Rms energy spread [MeV]	Full energy spread [MeV]
$s_s=4\text{mm}$ rms bunch length	9.2	3.6	14.8 (+/- 7.4)

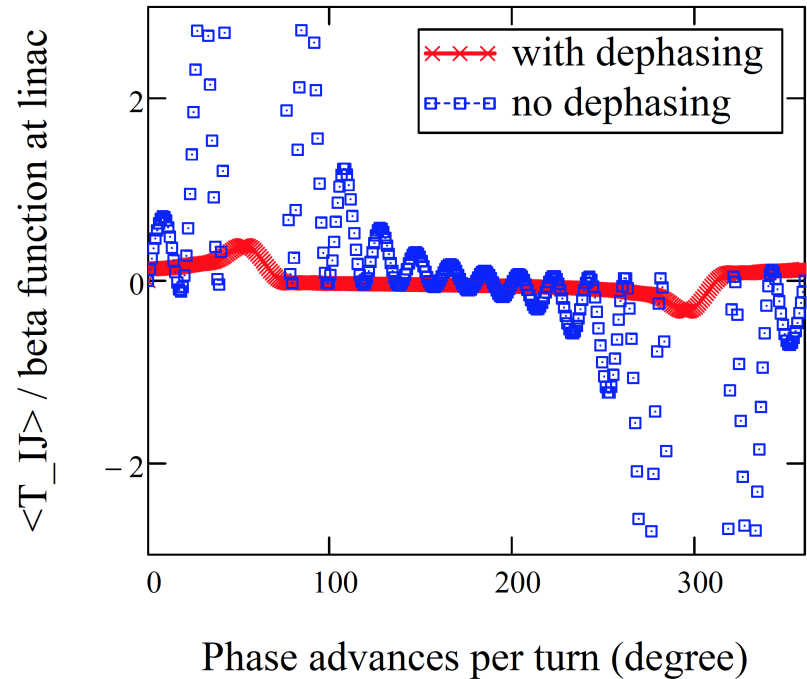
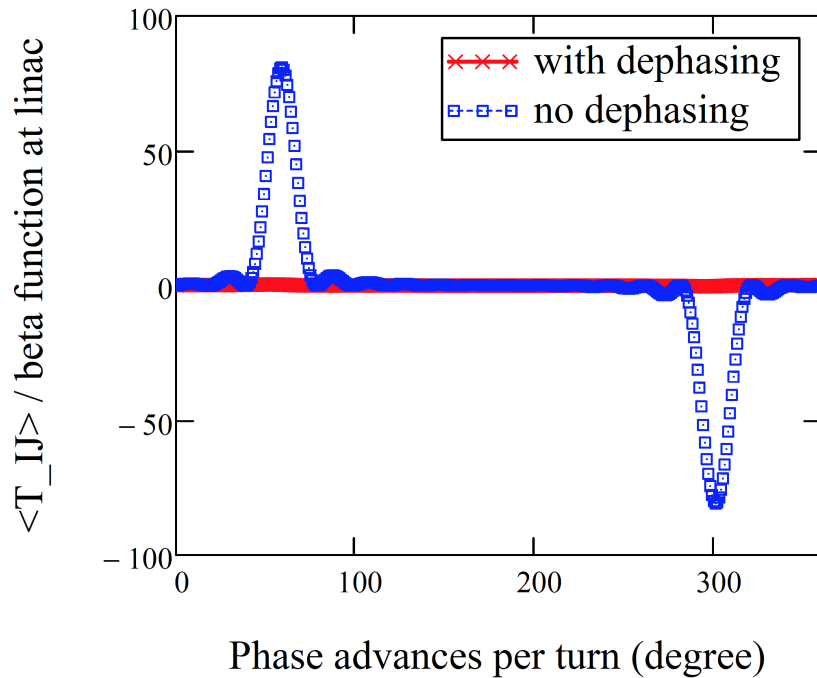
Energy spread
Resulting from SR
(F. Meot):
0.5 MeV

Chromatic Dephasing Effects in BBU

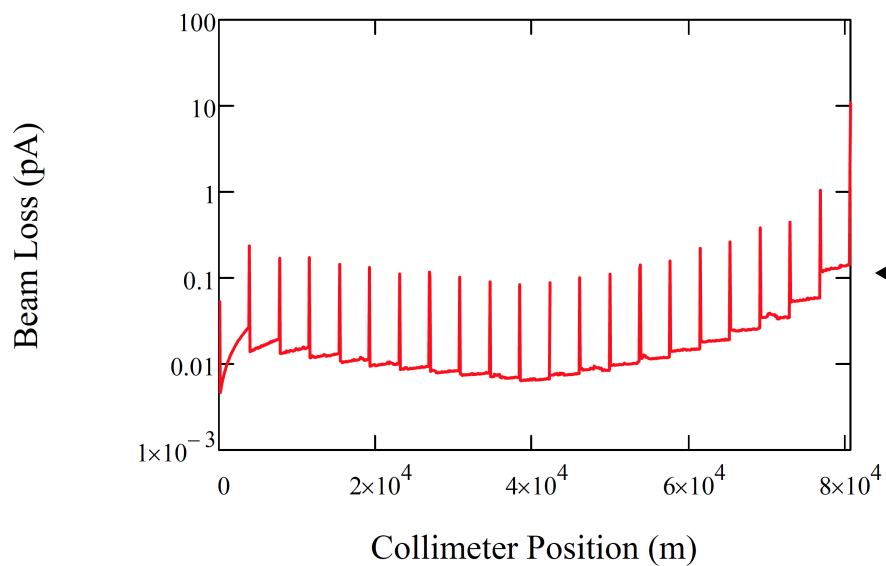
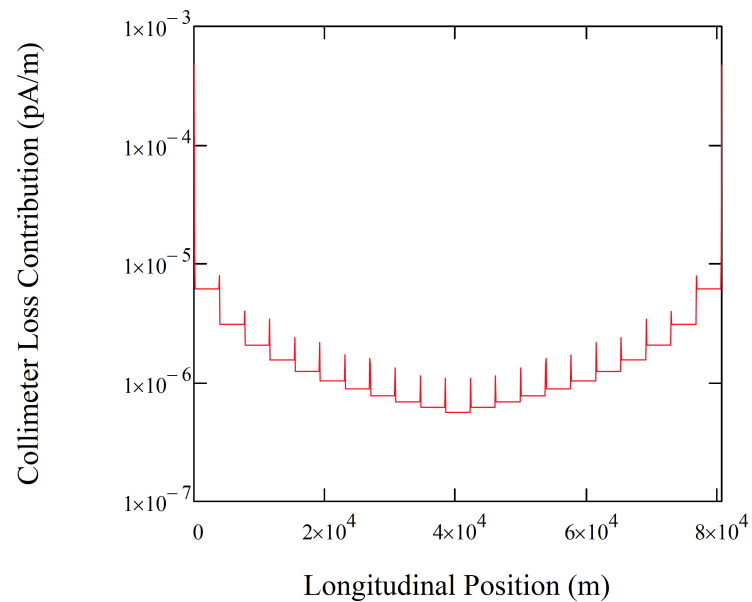
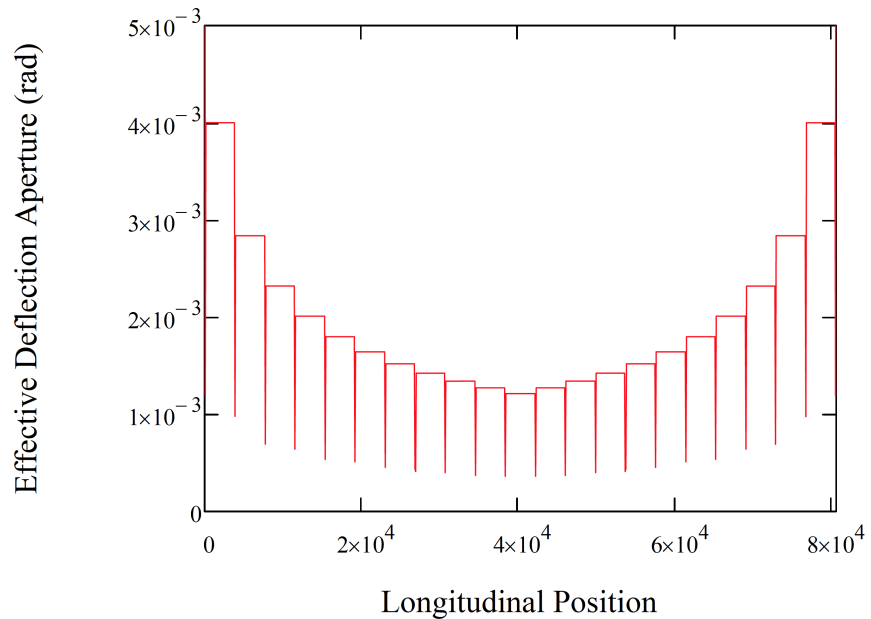
100* chromaticity



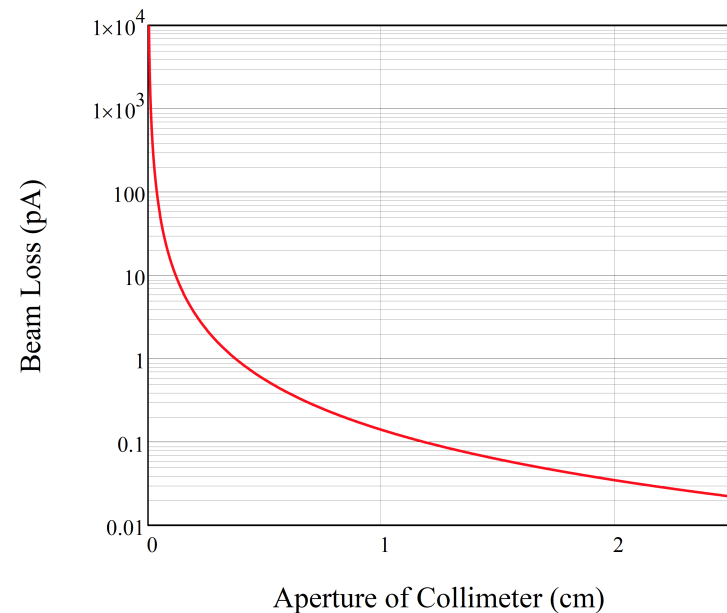
Chromatic Dephasing Effects in BBU 10000* chromaticity



Beam Losses Due to Elastic Scattering



← In last arc



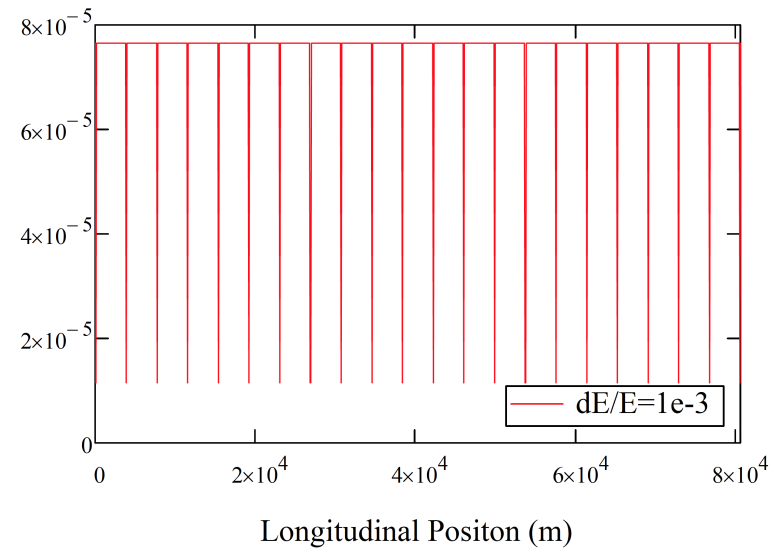
Beam Losses Due To Bremsstrahlung

$$\Delta E / E = 10^{-3}$$

Beam Loss Rate (pA/m)

$$\Delta E = 10 \text{ Mev}$$

@ last Linac Pass



Collimator Loss Contribution (pA/m)

